TURUN
YLIOPISTO
UNIVERSITY
OF TURKU

BLOOD PRESSURE AND HEMODYNAMIC MONITORING FROM THE FINGERTIP

Tuukka Panula

TURUN YLIOPISTON JULKAISUJA – ANNALES UNIVERSITATIS TURKUENSIS
SARJA – SER. F OSA – TOM. 41 | TECHNICA – INFORMATICA | TURKU 2024

TURUN
YLIOPISTO
UNIVERSITY
OF TURKU

BLOOD PRESSURE AND HEMODYNAMIC MONITORING FROM THE FINGERTIP

Tuukka Panula

TURUN YLIOPISTON JULKAISUJA – ANNALES UNIVERSITATIS TURKUENSIS
SARJA – SER. F OSA – TOM. 41 | TECHNICA – INFORMATICA | TURKU 2024

University of Turku

Faculty of Technology
Department of Computing
Information and Communication Technology
Doctoral Programme in Technology (DPT)

Supervised by

Assistant Professor, Matti Kaisti
Department of Computing
University of Turku
Turku, Finland

Professor, Pasi Liljeberg
Department of Computing
University of Turku
Turku, Finland

Professor, Teemu Niiranen
Department of Internal Medicine
University of Turku
Turku, Finland

Reviewed by

Professor, Tapio Seppänen
Center for Machine Vision and Signal Analysis
University of Oulu
Oulu, Finland

Professor, Ramakrishna Mukkamala
Swanson School of Engineering
University of Pittsburgh
Pittsburgh, USA

Opponent

Professor, Alex Casson
Department of Electrical and Electronic Engineering
University of Manchester
Manchester, UK

The originality of this publication has been checked in accordance with the University of Turku quality assurance system using the Turnitin OriginalityCheck service.

ISBN 978-951-29-9792-3 (PRINT)
ISBN 978-951-29-9793-0 (PDF)
ISSN 2736-9390 (PRINT)
ISSN 2736-9684 (ONLINE)
Painosalama Oy, Turku, Finland, 2024

UNIVERSITY OF TURKU
Faculty of Technology
Department of Computing
Information and Communication Technology
PANULA, TUUKKA: Blood Pressure and Hemodynamic Monitoring from the Fingertip
Doctoral dissertation, 127 pp.
Doctoral Programme in Technology (DPT)
July 2024

ABSTRACT

Hypertension, or high blood pressure (BP), is the most significant risk factor for cardiovascular disease – the leading cause of death in the world. Fortunately, when detected early, it is easily controlled with medication and lifestyle changes. The emergence of wearable technologies and the ongoing miniaturization of microelectronics has paved the way for new BP monitoring technologies.

In this thesis, a collection of sensing modalities is experimented with and refined incrementally. Both the physical properties of the sensors and the underlying physiological phenomena are studied, providing deeper understanding into the mechanics of BP instrumentation. The key elements of this thesis are the extensive human studies that are conducted to demonstrate the capabilities and prove the reliability of the technologies.

This thesis introduces a new way of measuring BP from the fingertip. The technology is based on tono-oscillometry, where arterial pulsations are recorded while simultaneously applying controlled pressure to the finger. Cost-efficiency was achieved by using commercial pressure sensors and modifying them for the intended use. The underlying mechanisms were studied through mathematical modeling and sensor characterization. After validating the prototype in a preliminary human study, the technology was miniaturized with clinical translatability taken into account. The small form factor system was validated in a separate human study. Continuous BP monitoring was achieved by adding an optical sensing modality to the tono-oscillometric method. Using the non-pulsatile components in the photoplethysmogram signal, we were able to measure continuous BP with the low-frequency vascular unloading technique.

The methods and results from this study give new insights into the monitoring of BP and other hemodynamic parameters. The proposed technologies pave the way towards less intrusive bedside patient monitoring and increased user comfort – helping both patients and healthcare professionals.

KEYWORDS: Blood pressure, medical instrumentation, wearable electronics, oscillometry, tonometry

TURUN YLIOPISTO
Teknillinen tiedekunta
Tietotekniikan laitos
Tietotekniikka
PANULA, TUUKKA: Blood Pressure and Hemodynamic Monitoring from the Fingertip
Väitöskirja, 127 s.
Teknologian tohtoriohjelma
Heinäkuu 2024

TIIVISTELMÄ

Hypertensio eli korkea verenpaine on merkittävin sydän- ja verisuonitautien riskitekijä. Tarpeeksi ajoissa havaittuna hypertensiota voidaan kuitenkin hoitaa tehokkaasti lääkityksellä ja elämäntapamuutoksilla. Mikroelektroniikan kehitys ja kannettavien teknologioiden murros ovat mahdollistaneet uudenlaisten verenpaineen seurantamenetelmien kehityksen.

Tässä väitöstyössä tutkitaan verenpaineen instrumentoinnin menetelmiä. Paneutumalla antureiden fysikaalisiin ominaisuuksiin ja niiden mittaamiin fysiologisiin ilmiöhin tavoitellaan verenpaineen mittausmenetelmien toiminnan syvällistä ymmärrystä. Keskeisessä osassa väitöskirjaa ovat kliiniset kokeet, joiden avulla osoitetaan teknologioiden kyvykkyys ja luotettavuus.

Väitöstyö esittelee uuden menetelmän verenpaineen mittaamiseen sormenpäästä. Tämä teknologia perustuu kehittämäämme tono-oskillometriseen menetelmään, jossa valtimon pulsaatiota mitataan samalla, kun sormeen kohdistetaan kontrolloitu paineenmuutos. Kustannustehokkuutta tavoiteltiin käyttämällä kaupallisia paineantureita, joita muokattiin tähän käyttöön sopiviksi. Vaikuttavia mekanismeja tutkittiin sekä matemaattisen mallinnuksen että antureiden sähköisen karakterisoinnin avulla. Kehitettyä teknologiaa hyödyntävä prototyyppilaite validoitiin alustavassa ihmiskokeessa. Laitteen soveltuvuutta kliiniseen käyttöön parannettiin miniatyrisoimalla aiemman instrumentin mekatroninen toteutus. Sormenpäähän kiinnitettävä instrumentti validoitiin erillisessä kliinisessä kokeessa. Laitetta kehitettiin edelleen jatkuva-aikaiseen verenpaineenseurantaan sopivaksi lisäämällä tähän optinen anturiyksikkö. Hyödyntämällä fotoplethysmogrammisignaalin vakiovirtakomponentteja yhdessä takaisinkytketyn paineensäädön kanssa, saavutettiin tarkka veren keskipaineen seuranta. Tämän niin kutsutun matalataajuisen tilavuuskompensaatiomenetelmän toimivuus todennettiin erillisessä ihmiskokeessa.

Tässä väitöskirjassa esitellyt menetelmät ja tulokset tarjoavat uusia näkemyksiä verenpaineen ja muiden hemodynaamisten parametrien seurantaan. Esitetyt teknologiat edistävät kajoamattoman potilasmonitoroinnin kehitystä ja lisäävät käyttäjämukavuutta – hyödyttäen näin sekä potilaita että terveydenhuollon ammattilaisia.

ASIASANAT: Verenpaine, lääketieteellinen instrumentointi, puettava elektroniikka, oskillometria, tonometria

Acknowledgements

Finishing this thesis would not have been possible without a multitude of people helping me on this journey. I express my deepest gratitude to all those who have supported me in the preparation of this dissertation.

I am grateful to my supervisors, Professor Pasi Liljeberg and Professor Teemu Niiranen, for their dedicated assistance and insightful advice throughout this research. Special thanks to my primary supervisor, Assistant Professor Matti Kaisti, for his invaluable support, guidance, and encouragement throughout this research.

My heartfelt thanks go to the amazing research group I have had the opportunity to work during these years. I would like to thank my coauthors Dr. Mikko Pänkäälä and Tero Koivisto for their guidance and scientific support. Professor Ilkka Kantola and research nurse Essi Roine from Turku university hospital have made the thesis possible through their expert management of the clinical aspects of this study. Especially, I would to thank Jukka-Pekka Sirkiä for his help in developing the instrumentation during the project and providing valuable scientific insights. In addition, I would like to thank Dr. Benny Lo from Imperial College London for his guidance during my research visit.

I would like to acknowledge the reviewers, including Professor Tapio Seppänen and Professor Ramakrishna Mukkamala, for their expert assessments and thoughtful recommendations that contributed to the final version of this dissertation. I am most grateful for Professor Alex Casson for his willingness to make the travel from Manchester to Turku and honored to have him as the opponent.

I owe a great debt of gratitude to my family for their unwavering support and understanding during the highs and lows of this journey. My parents, Leila and Jorma as well as my grandparents, Tuula and Ahti have always been my biggest supporters. I would also like to thank my siblings Iiris and Elias and all my friends for rooting for me on the way. Finally I would like to thank my beloved Oona for standing by me during the whole process and even willing to move to London with me for six months. I would not be here if it weren't for you.

July 8th 2024

Tuukka Panula

TUUKKA PANULA

Tuukka Panula received the B.Sc. (Tech.) degree in computer and electronics engineering and the M.Sc. (Tech.) degree in health technology from the University of Turku, Turku, Finland, in 2018 and 2019, respectively. From 2022 to 2023, he was with the Hamlyn Centre for Robotic Surgery, Imperial College London, London, U.K., where he worked as a visiting Ph.D. researcher for six months. Panula is currently a university teacher at the University of Turku, lecturing courses on medical instrumentation and health technology.

Table of Contents

Acknowledgements . . . . . **vi**

Table of Contents . . . . . **viii**

Abbreviations . . . . . **x**

List of Original Publications . . . . . **xii**

1 Introduction **1**

2 Literature review **4**

2.1 Principles of Blood Pressure Measurement Techniques . . 4

2.1.1 Manual auscultation 6

2.1.2 Oscillometric method 7

2.1.3 Tonometry 8

2.1.4 Pulse wave propagation 10

2.1.5 Pulse wave morphology 11

2.1.6 Vascular Unloading Technique 12

2.1.7 Differential oscillometry 13

2.1.8 Sources of inaccuracy 13

2.2 Recent advances and validation in blood pressure instruments 14

2.2.1 Miniaturization of cuff oscillometry 15

2.2.2 Oscillometric finger pressing method 17

2.2.3 Tonometry 17

2.2.4 Pulse propagation methods 18

2.2.5 Pulse wave morphology 19

2.2.6 Transdermal optical imaging 20

2.3 Modeling and algorithms 20

2.3.1 Physiological models 22

2.3.2 Machine learning 24

2.4 Summary of the literature review 25

3 Aims of the study **27**

4 Materials and Methods **29**
4.1 Reference instruments for hemodynamic monitoring 29
4.2 Other equipment 30
4.3 Software and firmware 30
4.4 Human studies 30
4.4.1 Human study I 30
4.4.2 Human study II 31
4.4.3 Human study III 31
4.4.4 Human study IV 32

5 Summary of the results **34**
5.1 Wearable pressure sensing array 34
5.1.1 Electrical characterization 34
5.1.2 Comparison to invasive arterial waveform 36
5.1.3 Atrial fibrillation 37
5.2 Automated tono-oscillometry 38
5.2.1 Sensing principle 38
5.2.2 Algorithm 40
5.2.3 System design 42
5.2.4 Validation 44
5.2.5 Modeling 48
5.3 Continuous BP monitoring 48
5.3.1 Low-frequency vascular unloading technique 49
5.3.2 Vasomotor compensation 50
5.3.3 Blood pressure measurements 51

6 Discussion **53**
6.1 Achievement of the aims 53
6.2 Technological feasibility of fingertip BP monitoring 54
6.3 Future directions 55

7 Conclusion **56**

List of References **58**

Original Publications **71**

Abbreviations

AAMI	Association for the Advancement of Medical Instrumentation
AC	Alternating Current
AF	Atrial Fibrillation
AP	Augmentation Index
ASIC	Application-Specific Integrated Circuit
ASI	Arterial Stiffness Index
BHS	British Hypertension Society
BP	Blood Pressure
CAD	Computer-Aided Design
CASP	Central Arterial Systolic Pressure
CBP	Central Blood Pressure
CAD	Computer-Aided Design
CBP	Central Blood Pressure
CAD	Computer-Aided Design
CNAP	Continuous Noninvasive Arterial Pressure
DLS	Dynamic Light Scattering
DBP	Diastolic Blood Pressure
DC	Direct Current
ECG	Electrocardiography
EDA	Electronic Design Automation
ESH	European Society of Hypertension
FDM	Fused-Deposition Modeling
FFT	Fast Fourier Transform
GUI	Graphical User Interface
HR	Heart Rate
I^2C	Inter-Integrated Circuit
IDE	Integrated Development Environment
ISO	International Organization for Standardization
ITP	Intra-Thoracic Pressure
LED	Light-Emitting Diode
MAP	Mean Arterial Pressure
MCU	Microcontroller Unit
MEMS	Micro-Electro-Mechanical System

MLR	Multivariate Linear Regression
mmHg	Millimeters of Mercury
OMWE	Oscillometric Waveform Envelope
PAT	Pulse Arrival Time
PDA	Pulse Decomposition Analysis
PEP	Pre-Ejection Period
PID	Proportional-Integral-Derivative
PLR	Passive Leg Raising
PTT	Pulse Transit Time
PWV	Pulse Wave Velocity
PWA	Pulse Wave Analysis
SBP	Systolic Blood Pressure
SD	Standard Deviation
SLS	Selective Laser Sintering
SVR	Support Vector Regression
TOI	Transdermal Optical Imaging
UART	Universal Asynchronous Receiver-Transmitter
USB	Universal Serial Bus
VCT	Volume Control Technique
VUT	Vascular Unloading Technique
WHO	World Health Organization

List of Original Publications

This dissertation is based on the following original publications, which are referred to in the text by their Roman numerals:

I Kaisti, M., Panula, T., Leppänen, J., Punkkinen, R., Jafari Tadi, M., Vasankari, T., ... & Pänkäälä, M. (2019). Clinical assessment of a non-invasive wearable MEMS pressure sensor array for monitoring of arterial pulse waveform, heart rate and detection of atrial fibrillation. NPJ digital medicine, 2(1), 39.

II Panula, T., Koivisto, T., Pänkäälä, M., Niiranen, T., Kantola, I., & Kaisti, M. (2020). An instrument for measuring blood pressure and assessing cardiovascular health from the fingertip. Biosensors and Bioelectronics, 167, 112483.

III Panula, T., Sirkiä, J. P., & Kaisti, M. (2023). Continuous Blood Pressure Monitoring using Non-Pulsatile Photoplethysmographic Components for Low-Frequency Vascular Unloading. IEEE Transactions on Instrumentation and Measurement.

IV Panula, T., Sirkiä, J. P., Koivisto, T., Pänkäälä, M., Niiranen, T., Kantola, I., & Kaisti, M. (2023). Development and clinical validation of a miniaturized finger probe for bedside hemodynamic monitoring. Iscience, 26(11).

V Kaisti, M, Panula, T., Sirkiä, J. P., Pänkäälä, M., Koivisto, T., Niiranen, T., & Kantola, I. (2024). Hemodynamic Bedside Monitoring Instrument with Pressure and Optical Sensors: Validation and Modality Comparison. Advanced Science, in publication.

Contributions of the author:

I Performed the electrical characterization of the sensor, participated in analyzing the data and writing the manuscript.

II Conceived the idea, developed the sensing technology, instrument and algorithms, analyzed the data, performed the human study and wrote the manuscript.

III Conceived the idea, developed the sensing technology, instrument and algorithms, analyzed the data, performed the human study and wrote the manuscript.

IV Conceived the idea, took part in developing the instrument, developed the algorithms, analyzed the data, took part in performing the human study and wrote the manuscript.

V Participated in developing the instruments, analyzing the data, performing the human studies and writing of the manuscript.

1 Introduction

Hypertension – or high blood pressure (BP) – is a health burden that affects more than a billion people globally [1]. It is a serious medical condition that markedly elevates the risk of potentially life-threatening cardiovascular diseases, including heart failure, coronary artery disease, and stroke. Sub-optimal blood pressure (BP) remains the foremost global risk factor for the overall burden of disease, resulting in over 10 million deaths and the loss of 212 million healthy life years annually. [2] Simultaneously, hypertension is the most common preventable risk factor for cardiovascular disease [3]. Fortunately, diagnosed hypertension can be well controlled via medication and lifestyle alterations. Nevertheless, the condition is mostly asymptomatic, and fewer than 20% of individuals with hypertension effectively manage it. [1]. Proper blood pressure (BP) control has been demonstrated to significantly reduce cardiovascular morbidity and all-cause mortality associated with hypertension [4]. Therefore, regular and accurate BP measurements are crucial for the successful prevention and treatment of hypertension [5; 6]. The significance of hypertension management is underscored by the increasing strictness of thresholds for high BP in recent clinical guidelines. According to recent hypertension guidelines, a systolic BP (SBP) of $\geq$ 120 mmHg with a diastolic BP (DBP) of $<$ 80 mmHg is classified as elevated BP. Readings exceeding 130 mmHg or 80 mmHg for SBP and DBP, respectively, fall into the category of Stage I hypertension [7].

Traditionally BP has been measured intermittently, providing ”snapshots” into the person's cardiovascular health. Recently, there has been a growing interest in the development of non-invasive techniques for the convenient and accurate monitoring of BP, allowing for the tracking of long-term changes and provides personalized actionable information. While self-monitoring at home has become commonplace, telemonitoring, where BP readings are transmitted to the patient's physician, remains fairly uncommon [8]. Technological advancements in BP monitoring include the use of modern digital sensors and devices, integration with machine learning techniques, the development of wearable solutions, continuous BP monitoring, and integration into digital health ecosystems.

BP can be taken invasively or non-invasively. Arterial cannulation, being an invasive technique, is mostly reserved for use in intensive care settings and is not suitable for home use. Since the 1970's efforts have been made to introduce automated non-invasive monitoring to the wider public [9]. Non-invasive BP mea-

surement techniques can be divided into two coarse categories: direct and indirect measurement. Direct measurement techniques use pressure sensors, possibly along with other sensing modalities, to measure the actual pressure withing the artery. For example, the oscillometric technique and applanation tonometry, while being non-invasive, attempt to probe the intra-arterial pressure directly. In contrast, indirect methods, such as pulse propagation methods and pulse morphology analysis, use features that are known to correlate with BP and its changes. These metrics can be translated into BP via dedicated mathematical models. Advances in machine learning and artificial intelligence have paved the way for new analysis techniques in BP monitoring.

The validation of BP monitors has been recently under scrutiny. The emergence of new cuffless methods, involving continuous operation and requiring additional calibration, has raised questions on the eligibility of existing validation standards. While designing new sensing modalities, it is important to keep track of recent developments in the field of standardization.

This thesis focuses on the development, implementation and validation of pressure sensor based BP monitoring technologies. The thesis involves the design of both the hardware as well as the algorithmic and signal processing aspects of the system development. The physical properties of the sensors and the underlying physiological phenomena are studied via mathematical modeling and sensor characterization. In addition to BP, we study how additional hemodynamic parameters can be extracted using the proposed technology. The technologies are finally verified in separate clinical trials. The thesis is comprised of a collection of five independent journal articles.

The first article introduces a miniature pressure sensor array, which is used to record radial artery pressure waveform. The study was made in collaboration with Murata Electronics Oy. The sensor development was made at Murata, and the sensor characterization as well as the clinical study and data analysis was done at the University of Turku. [10]

In the second article, we proposed a new method for measuring BP and other hemodynamic variables from the fingertip [11]. A table-top instrument with a custom sensor and mechatronics was proposed. The study resulted in a blood pressure sensing system that was based on a modified commercial pressure sensor. A clinical study (n=33) for validating the design was conducted in collaboration with the Turku University Hospital. Part of the results were also published in conference proceedings [12].

The third article uses the same principles introduced in the second article, but in a miniaturized form factor [13]. In addition to the pressure sensor, an optical sensor is integrated to the device. A new low-frequency vascular unloading method for measuring continuous BP was proposed. A compensation method for vasomotion was also proposed. A proof-of-concept human study was performed. Part of the results were also published in conference proceedings [14].

The fourth article is based on the same miniaturized sensor system developed for the third article [15]. The goal of the study is to refine the sensing technoloqy into a wearable finger-worn form factor. The miniaturization process is represented in detail and the developed instrument is validated in a clinical study. Part of the results were also published in conference proceedings [16].

The fifth article combines the technologies and validation of studies II and IV, as well as an additional optical sensing technology introduced in [17]. With the combined analysis of the previous results, we are able to draw new conclusions and delve deeper into the mechanics of BP measurement.

This thesis is organized as follows. In chapter 2, the current literature is reviewed and the basic phenomena relating to BP and its monitoring are explained. Chapter 3 describes the aims of the original publications. Chapter 4 summarizes the materials and methods used. Chapter 5 summarizes the results of the four journal articles and delves deeper into the developed technologies. In chapter 6, the findings from the studies and future prospects are discussed. Chapter 7 finally concludes the study.

2 Literature review

Several reviews on blood pressure monitoring have been conducted, with some focusing on pulse propagation-based blood pressure estimation [18; 19], while others provide in-depth surveys on the fundamental principles of blood pressure measurement [20; 21]. In this chapter, we present a narrative review that delves into recent evidence concerning the technological maturity of both established and emerging technologies and instruments, with a particular emphasis on clinical validation.

Our inclusion criteria prioritize recent studies introducing novel techniques, algorithms, or instrument types. Preference is given to studies with robust clinical validation, although noteworthy proof-of-concept investigations are also considered when introducing innovative concepts. Additionally, we provide summaries of the primary blood pressure (BP) measurement principles as well as ongoing commercial initiatives.

This chapter is based on a review article published in IEEE Reviews in Biomedical Engineering in 2022 [22].

2.1 Principles of Blood Pressure Measurement Techniques

Blood pressure (BP) is typically expressed as two values: systolic (SBP) and diastolic (DBP) readings. The heart ejects the blood into the circulatory system, generating a pulsatile pressure gradient that travels along the blood vessels, creating a pulse wave. SBP represents the maximum value reached by the pressure waveform during systole (the heart muscle contraction phase), while DBP is the minimum value observed during diastole (the interval between contractions). Pulse pressure (PP) is the difference between SBP and DBP within a single cardiac cycle. The cardiac pulse refers to the pressure cycle between two consecutive minimums, known as diastolic feet, in the pulse. Mean arterial pressure (MAP) denotes the average pressure over one cardiac cycle and can be computed from the arterial waveform by dividing the area under a single cardiac cycle by its duration [23]. Due to diverse physiological factors, such as blood vessel compliance (Windkessel effect), the prevailing BP varies across different segments of the cardiovascular system [23], as illustrated in Figure 1.

The arterial pulse wave is actually a combination of the initial wave from the

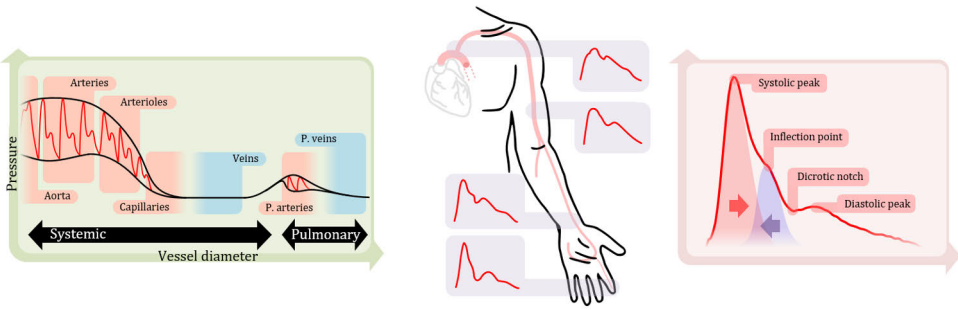

Figure 1. Basics of BP. Left: BP across different points in the circulatory system. Pressure reaches its peak as blood exits the left ventricle and traverses the major arteries. Upon entering the arterioles, the pressure drops significantly, maintaining a low level in the capillaries and veins. Subsequently, pressure increases upon entering the right side of the heart, propelling blood into the pulmonary circulation. Once again, pressure decreases in the pulmonary capillaries, and the blood, now oxygenated, enters the left atrium via pulmonary veins before being ejected into the systemic circulation. Middle: Due to wave reflection and the impact of arterial compliance, the pulse wave morphology exhibits changes as blood courses through the arteries. Right: The arterial pulse results from the superposition of distinct waves, with the initial systolic wave reflecting from high-resistance blood vessels. The inflection point's location indicates the velocity of the traveling wave, offering insights into arterial compliance and elasticity. Figure adapted from [22].

heart and its reflections as seen in Figure 1. The traveling arterial pulse wave gets deformed due to wave reflection from high resistance vessels. The more elastic the arteries are, the more the PP is amplified in the peripheral arteries. Correspondingly, the PP remains the same (and usually high) in very stiff arteries throughout the vessel [24].

When BP is discussed, the systolic and diastolic readings typically refer to the the pressure in large systemic arteries. It is most commonly measured in the brachial artery using an arm cuff [23], partly due to it's location at heart level and partly due to easy access. However, the BP in other parts of the body differs significantly from the brachial pressure. The hydrostatic effect does not affect brachial artery readings, but when BP is measured from other locations (e.g. wrist or fingers) large deviations may be seen [25]. In systemic circulation the heart has to deliver enough pressure to ensure sufficient tissue perfusion in the whole body, which results in relatively high BP throughout the systemic arteries. On the other hand, in pulmonary circulation the pressure is significantly lower. Even in the systemic circulation, the BP varies from the high pressure arteries to lower pressure arterioles and microcirculation before reaching the very low pressure veins. The arterioles are responsible for the largest pressure drop and resistance in the circulatory system. Although capillaries have clearly smaller diameter, indicating even higher resistance, their total cross-sectional area is much larger thus resulting in lower resistance relative to the arterioles.

Vasodilation and vasoconstriction, e.g. the active opening and narrowing, of

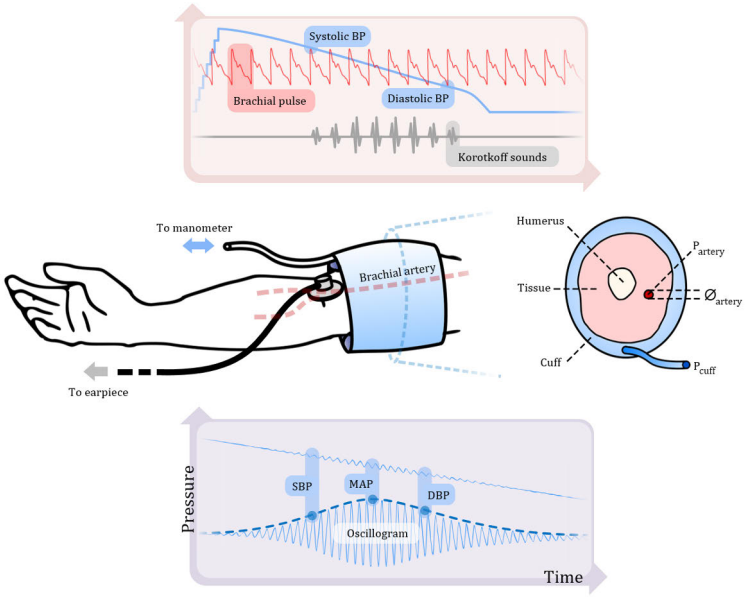

Figure 2. BP measurement via brachial cuff using manual auscultation (top) and oscillometric method (bottom). In both methods, an air-filled cuff is secured around the arm and inflated to a pressure above systolic levels before gradually releasing the pressure. The cuff is connected pneumatically to either a mercury manometer or an automated BP instrument. For the manual auscultation technique, a healthcare professional positions a stethoscope on the brachial artery, just below the cuff. The clinician listens for distinct Korotkoff sounds that correspond to the appearance and disappearance of sounds, indicating SBP and DBP respectively. Figure adapted from [22].

the arterioles have a significant role in regulating the BP to ensure low pressure in the capillaries. [26; 23] In doing so, the velocity of blood flow is reduced to allow sufficient time for gas and nutrient exchange [26], while providing enough perfusion pressure. In veins, the flow is nearly non-pulsatile except in the large veins proximal to the heart, such as the internal and external jugular veins [26]. This pressure-diameter relationship is described in Figure 1.

2.1.1 Manual auscultation

Manual measurement is regarded as the most precise non-invasive technique for evaluating blood pressure (BP), serving as the reference standard in international protocols [27]. However, manual auscultation only provides an approximation of true BP since it is not directly measured within the arterial lumen through cannulation. Despite its age, this technique persists in clinical practice and international validation standards. Originating in 1896 with the work of the Italian physician Scipione Riva-Rocci [28], the method involves using a mercury-filled sphygmomanometer

connected to a brachial cuff for systolic blood pressure (SBP) measurement. The cuff's pressure is manually pumped to a level exceeding SBP, rendering the radial pulse impalpable. Subsequently, the cuff is gradually deflated, and the radial pulse is palpated. The reading of SBP is determined when the pulse is detectable again, observed from the column of mercury in the sphygmomanometer. The unit mmHg (millimeters of mercury) persists due to the widespread and prolonged use of mercury sphygmomanometers. One mmHg is approximately equivalent to 133 Pa. [29]

The method introduced by the Russian military physician Nikolai Korotkoff expanded upon Riva-Rocci's auscultation technique [28]. Instead of palpating the radial artery, a stethoscope is positioned over the brachial artery while the cuff is deflated from supra-systolic pressure. When tapping sounds, known as Korotkoff sounds, become audible to the listener due to the turbulent flow of blood under external compression, systolic blood pressure (SBP) is recorded from the sphygmomanometer. The sounds persist during cuff deflation and cease when the cuff pressure aligns with the diastolic blood pressure (DBP). The procedure is illustrated in Figure 2. Manual auscultation and palpation techniques present challenges as they demand a skilled clinician and are susceptible to operator bias [21]. Additionally, the use of highly toxic mercury in sphygmomanometers has led to restrictions in many countries. Alternatives, such as aneroid sphygmomanometers and automated blood pressure monitors, are now recommended for clinical use by the World Health Organization [30]. These instruments include aneroid sphygmomanometers and digital devices that emulate a mercury column with an LCD display. Proper calibration and verification are essential to ensure their performance is akin to that of mercury devices.

2.1.2 Oscillometric method

The oscillometric method the predominant noninvasive technique for BP measurement, widely adopted by manufacturers of BP monitors. While the phenomenon was initially observed in the 19th century, its widespread use only realised with the advent of digital electronics [23]. In contrast to the manual auscultation method, which extracts both SBP and DBP, the oscillometric method directly measures only one value, the mean arterial pressure (MAP). SBP and DBP are only approximated from the acquired data.

In this approach, a cuff is positioned around the upper arm, encompassing the brachial artery. As the cuff pressure rises to suprasystolic pressure (beyond SBP), blood flow is completely obstructed. Upon release, the amplitude of pulsations – sometimes called oscillations – within the cuff increase until the cuff pressure is equal to the MAP. Subsequently, as the cuff pressure further decreases below the MAP, the pulsations start diminishing. Through signal processing, a bell-shaped curve, known as the oscillometric envelope (OMWE), is computed in the time do-

main, alongside the corresponding deflation curve [31]. In the conventional method, SBP and DBP are then derived from the MAP using predetermined percentages obtained from population studies (e.g., 50% and 80% of the MAP) by mapping these points to the cuff pressure curve [25; 21].

Oscillometric devices exhibit a certain level of uncertainty, as indicated by the recommendations in the US Association for the Advancement of Medical Instrumentation (AAMI) standard. The standard permits standard deviation (SD) of $\pm$ 8 mmHg compared to manual auscultation, which can often surpass the typical in-person blood pressure (BP) variability [27]. This uncertainty is particularly pronounced in the commonly used fixed ratio method [32], and discrepancies become more apparent when arterial compliance and pulse pressure deviate significantly from typical levels.

Various approaches have been suggested to enhance the fixed ratio method in oscillometry [25]. A straightforward yet effective method involves identifying the pressure where the oscillogram envelope exhibits the steepest slopes. However, accurate BP estimation with this method requires low-noise measurements [33]. Other solutions include patient-specific modeling [34; 35], the application of neural networks, and pulse morphology analysis [25]. Integrating additional data into oscillometric BP estimates has also been proposed to enhance reliability [36]. BP fluctuations in the continuous arterial pulse waveform are employed to estimate potential outlier readings [37].

In a recent study with a sample size of 20, the optimal measuring sites (upper arm, middle forearm, wrist, finger proximal phalanx, and finger distal phalanx) for cuff-based oscillometry were explored. The study concluded that the finger's distal phalanx was the second-best site after the upper arm. The reported differences between finger and upper arm measurements were ((mean $\pm$ standard deviation) mmHg) (-2.34 ± 6.82) mmHg, (-6.7 ± 12.9) mmHg, and (1.7 ± 8.7) mmHg for MAP, SBP, and DBP, respectively [37].

2.1.3 Tonometry

The principle behind tonometry originates from one of the most basic tools in medicine - palpating the pulse. However, in tonometry, the output can be recorded and quantified by an instrument called a tonometer. A traditional applanation tonometer is a handheld pen-like device with a pressure-sensitive tip that is placed over an artery, as illustrated in Figure 5 [38]. Similar to manual palpation, tonometry is based on applying external pressure perpendicular to the artery.

Various types of arterial tonometers have been available for a long time, and early devices using the same principle were in use in the 19th century [23]. Nevertheless, the technology is susceptible to motion artifacts, incorrect placement, and changes in counter pressure. Correct applanation pressure is achieved when the external pres-

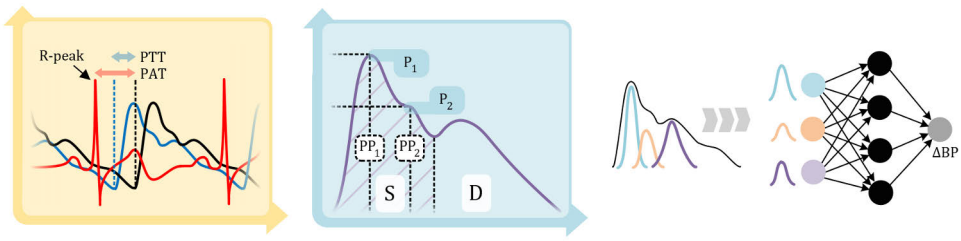

Figure 3. Left: Distinction between pulse transit time (PTT) and pulse arrival time (PAT). PTT measures the time interval between two pulses recorded at different locations, often using PPG. PAT, on the other hand, measures the duration it takes for the pulse to propagate from the heart to a peripheral artery, such as the finger. It is computed from the R-peak of the ECG tracing to the peripheral systolic wave. Middle: Pulse wave analysis (PWA). Features derived from the pulse waveform include pulse pressures, denoted as PP_1 and PP_2, at specific points P_1 and P_2, along with systolic and diastolic areas (S and D). Right: Pulse decomposition analysis (PDA). The individual components of a cardiac pulse are segmented into wavelets, allowing them to be processed by a machine learning algorithm to evaluate changes in blood pressure (BP). Figure adapted from [22].

sure from the tonometer equals the pressure (P_i) inside the artery, i.e., the mean arterial pressure (MAP). This ensures maximum pressure coupling to the sensor.

In applanation tonometry, the external pressure (P_e) is applied perpendicular to the tube surface and matched with the MAP. Thus, the transmural pressure (P_t) equals zero. Since the external pressure is kept constant, the transmural pressure is strictly zero only when the BP pulse is at the MAP. The tube, or the artery, is almost completely flattened, and the radius r can be thought to approach infinity perpendicular to the external force vector. Then, all pressure is directed both to the tonometer and the underlying stiff surface, usually bone. The principle can be summarized as:

$$P_t = P_i - P_e = \frac{\mu \cdot T}{r} \overset{r \to \infty}{\to} 0, \tag{1}$$

$$P_i = P_e, \tag{2}$$

where T is wall tension, and μ is wall thickness [24]. This way, the pressure applied and consequently measured by the tonometer is equal to the internal pressure of the artery. If too little pressure is applied, the pressure coupling is insufficient, and with too much applied pressure, the artery is occluded, blocking blood flow. A common issue with pen-type tonometric instruments is that the technique is very sensitive to sensor misplacement and the applied force. Even the slightest hand tremor can mask the actual pulsation of the artery. The pressure values output by a tonometer are usually arbitrary and have to be calibrated to actual BP values using, for example, cuff oscillometry [38].

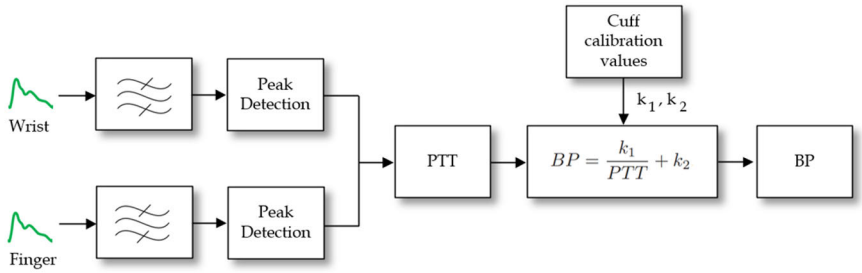

Figure 4. PTT analysis pipeline. Pulsewave is measured at two locations (e.g. the wrist and the finger). The signals are fed through band-pass filtering and peak detection. The time between the peaks of each signal is used to obtain PTT, which is then transformed into pressure using a simple equation. This value is calibrated into actual BP values.

2.1.4 Pulse wave propagation

Pulse wave propagation offers a method for estimating BP without the need for a cuff [20; 18; 19]. Typically assessed in terms of time or velocity, this approach requires a multimodal sensing setup. Common configurations involve electrocardiography (ECG) paired with photoplethysmography (PPG), or the use of two PPG sensors – one distal and one proximal. The generally used terms are pulse transit time (PTT) and pulse arrival time (PAT). PTT denotes the time required for the pressure wave to travel from a proximal arterial site to a distal one [18]. Pulse arrival time is used to describe the time from the ECG R-peak to the systolic peak of the proximal arterial pulse. Experimental studies have demonstrated a linear relationship between PTT and BP, expressed by the following model equation [18]:

$$BP = \frac{k_1}{PTT} + k_2, \tag{3}$$

where k_1 and k_2 serve as calibration parameters. Calibration is often done using traditional brachial cuff oscillometry. Various alternative models have been proposed [18], and investigations have explored models incorporating additional physiological parameters, such as heart rate [39]. A closely related concept is pulse wave velocity (PWV), computed by dividing the distance between the sensor locations by the difference in pulse arrival time at those locations [40]. Widely used in clinical practice, PWV is regarded as the gold standard non-invasive method for measuring arterial stiffness [41]. It has also been employed for indirect BP estimation [42; 40; 43] and demonstrated as an independent predictor of incident hypertension [44]. The Moens-Korteweg equation [45; 46], a commonly used physical model, establishes a relationship between the velocity of a pressure pulse and the elastic modulus of the artery through which the pressure pulse propagates [47].

Pulse wave propagation based BP measurement, if clinically validated, would allow for continuous and convenient BP monitoring. However, PTT/PAT based tech-

niques are limited by the need for calibration [18]. The calibration fits the model parameters, such as the ones in equation 3, using, e.g., pairs of measured PTT/PAT and BP values. Typically, a traditional cuff-based oscillometric BP measurement is used during initial calibration and possibly at regular intervals. Unsurprisingly, increasing the length of the calibration interval is associated with decreased BP estimation accuracy, although the decrease in accuracy might not always be so straightforward [48]. Consequently, the accuracy of long-term monitoring is a hindrance of this technique [49].

2.1.5 Pulse wave morphology

Various pulse wave morphology analysis techniques can extract BP information from the arterial pulse waveform. Hemodynamic phenomena resulting from BP and its alterations have a significant impact on the shape of the pulse. [50]. Pulse wave analysis (PWA) utilizes the features extracted from the pulse contour, illustrated in Figure 3. These features include, e.g., pulse pressure (PP), systolic and diastolic volumes, augmented pressure, and augmentation index (AIx). AIx is the ratio of the pulse pressure of the initial systolic peak (PP_1) to the PP at the inflection point caused by wave reflection (PP_2)[50]: $AIx = \frac{PP_2}{PP_1} \cdot 100(\%)$. In some devices, the peripheral pulse is transformed into aortic pulse via a generalized transfer function or a similar approach [24]. The obtained features can be entered into a mathematical model or a machine learning algorithm to calculate actual pressure measurements. To enhance accuracy, additional patient details such as age, weight, height, and sex can be incorporated. When utilized for BP monitoring, pulse wave analysis (PWA) methods typically require an initial calibration using a brachial cuff. Similar to pulse propagation methods, PWA is more suitable for estimating relative changes in blood pressure rather than absolute values. [50]

A similar approach, pulse decomposition analysis (PDA), is based on assessing the cardiac pulse contour [51; 52; 50]. PDA relies on analyzing the reflected waves observed in the arterial pulse waveform. The theory underlying PDA suggests that, apart from the primary systolic pulse, two pulses are reflected from two major reflection sites originating from the renal arteries and the iliac arteries, branching from the abdominal aorta. These reflections' characteristics and locations are influenced by blood pressure and flow velocity. By fitting this information into a model, changes in blood pressure can be estimated [51]. PDA technology can be valuable in detecting relative variations in blood pressure, but it requires initial calibration using techniques such as oscillometry. Further research is needed to fully comprehend the theory of major arterial reflection points. It remains uncertain to what extent changes in pulse morphology are caused by variations in reflection waves versus transmural pressure changes and positioning within the pressure-compliance curve. The principles of PDA are illustrated in Figure 3.

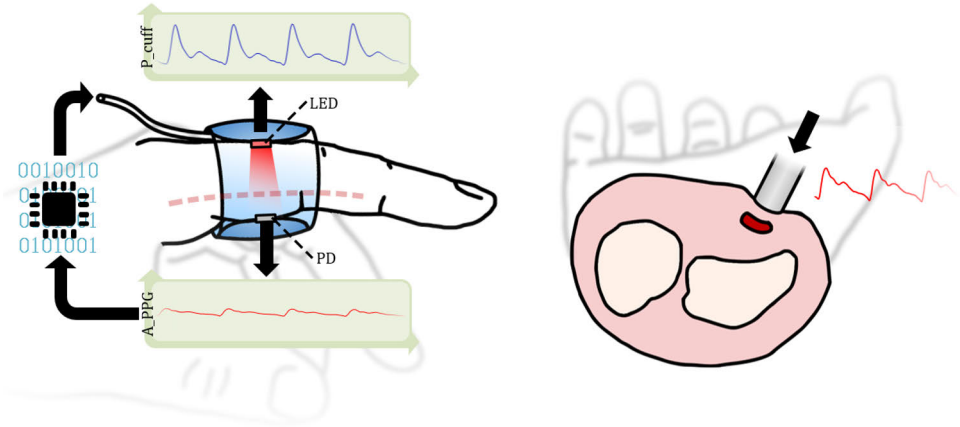

Figure 5. Left: Vascular unloading technique (VUT). A miniature cuff, incorporating a PPG unit, is positioned around a finger. A feedback system is employed to administer pulsatile counter pressure to the cuff, ensuring a constant optical blood flow signal. Consequently, the cuff pressure equals the intra-arterial pressure. Right: An illustration of arterial tonometry depicting a cross section of the arm with radial and ulnar bones, along with the radial artery. A pen-shaped tonometer is applied to the skin, exerting pressure on the artery. Changes in artery volume are captured through a pressure sensor. Figure adapted from [22].

2.1.6 Vascular Unloading Technique

The Vascular Unloading Technique (VUT) or volume clamp method was invented by the Czech physiologist Jan Penaz in 1973 [53; 54]. This method can be used for continuous beat-by-beat BP monitoring [53; 21]. A typical VUT system comprises a primary control unit and a finger cuff device connected by a combination of communication cables and pneumatic tubing. The main unit houses the pump and valves required for pneumatic pressure management. The finger cuff unit consists of a control unit worn on the wrist and one or two miniature air cuffs placed around the finger(s). The cuff has both a light emitting diode (LED) and a photodiode, much like a pulse oximeter. This optical PPG system observes the pulsatile blood volume in the artery by measuring the light transmitted through it. A VUT device utilizes a feedback control loop system that applies counter pressure to the cuff, ensuring the optical blood flow signal remains constant during each cardiac cycle. The feedback system requires a minimum of 30 Hz of bandwidth [53]. Different methods for finding an appropriate setpoint for the feedback system have been introduced, but there is no consensus on which is best single solution has been declared superior [55]. The feedback system in the VUT device adjusts the cuff pressure accordingly when there is an increase or decrease in optical blood volume. This mechanism ensures a constant volume in the artery and thus a constant ”flat” PPG reading. The continuously adjusted cuff, controlled by the feedback system, enables the reading of actual BP.

Additionally, VUT devices typically incorporate a traditional oscillometric brachial cuff into the system for initial calibration and periodic calibrations as needed. The finger cuff pressure signal is converted to an equivalent brachial BP via a transfer function. The technology is illustrated in Figure 5.

The Volume Control Technique (VCT) is an innovative approach introduced by CNSystems [56]. Similar to VUT, VCT operates on the principle of volume clamping. However, in contrast to full pulse contour clamping in VUT, VCT adopts a beat-wise clamping strategy. This involves integrating over each cardiac pulse within the optical feedback signal and adjusting cuff pressure to maintain a constant integral. Notably, VCT presents advantages over traditional VUT in terms of ease of implementation and miniaturization, as it eliminates the need for complex fast-switching pneumatics. The technology was successfully integrated into an existing VUT device through firmware customization. Initial tests involving 46 patients undergoing surgery showed promising results with a MAP of (-1.0 ± 7.0) mmHg. It is important to note that these encouraging findings are not yet validated through a standard protocol [56].

2.1.7 Differential oscillometry

Similar to VUT, differential oscillometry is a method for continuously unloading the artery by a feedback servo system [57]. It bears a resemblance to VCT in the way it controls the volume on a beat-to-beat level, not altering the pressure during the cardiac cycle. However, it does not use PPG concurrently with the finger pressure cuff. Instead two finger cuffs are held at similar pressures – one being slightly below MAP ($P_1 = P_{\text{mean}} - \epsilon$) and the other slightly above it ($P_2 = P_{\text{mean}} + \epsilon$). When the amplitude of both of these cuff pulsations are equal, the MAP can be found at halfway between the two pressures ($P_{mean} = \frac{P_1+P_2}{2}$). If this condition is not met, the feedback system adjusts the pressure until both cuffs exhibit the same pulse pressure. Differential oscillometry was implemented in the UT9201 device, and tested against arterial cannulation in 22 cardiac patients. The mean$\pm$SD for MAP was 2.7$\pm$4.9 mmHg [58]. Partly due to the technology being developed and used in the former Soviet economic area, it did not gain popularity in western academia.

2.1.8 Sources of inaccuracy

All the methods discussed above share two common characteristics: they are non-invasive and, therefore, inherently subject to a certain degree of inaccuracy. With the exception of intra-arterial cannulation, all blood pressure (BP) measurement techniques entail a possibility of error. International standards define the clinically acceptable limits of error [59]. The accuracy of a device needs to be assessed at a population level, rather than for individual measurements. Even a validated device

may provide highly incorrect readings for certain individuals, potentially resulting in a lack of appropriate treatment. Such individuals may fall into special population categories, where BP measuring devices validated with the general population might not be accurate. For instance, young children, pregnant women, and individuals with atrial fibrillation can be considered special populations [60; 59].

Manual auscultation is susceptible to listener bias and physiological factors, such as unclear or faint Korotkoff sounds. Interestingly, due to the nature of the mercury column scale, readings are often marked as even numbers, although this has a minor impact on accuracy.

The oscillometric method introduces a clear source of inaccuracy. It indirectly estimates SBP and DBP based on the shape of the oscillogram and MAP. Factors such as arterial compliance (stiffness of the arteries) can affect the shape of the oscillogram, distorting results. Incorrect cuff size, as well as large arm circumference (considered a special population for deriving validation standards for BP measuring devices), also significantly impact accuracy [59]. Common to all techniques relying on calibration, such as VUT, pulse morphology analysis, and pulse propagation methods, is the propagation of error introduced during the oscillometric calibration [23; 35].

Pulse wave propagation methods suffer from the inherent inaccuracy of equating one variable to another through a model. The duration for which the model remains valid post-calibration is another potential source of inaccuracies. Depending on the sensor setup used, pre-ejection period (PEP), and sensor contact force on the skin can also serve as confounding factors, as mentioned earlier.

Tonometry is susceptible to sensor misplacement, motion artifacts, and, when operated by a human, incorrect application pressure. Pulse wave morphology also suffers from inaccuracies caused by sensor misplacement and movement artifacts but even more so from the fact that blood pressure is estimated based on numerous features, and possibly also patient specific information, which work as an input to a more or less complex model. Additionally, reduced blood perfusion in the extremities can make signal acquisition challenging [23].

2.2 Recent advances and validation in blood pressure instruments

The technologies introduced in this chapter find applications in various commercial devices and research prototypes. Most of the technologies discussed have undergone validation against international standard protocols. The standards that have been relevant over the past decades are established by organizations such as the US Association for the Advancement of Medical Instrumentation (AAMI), the European Society of Hypertension Working Group on Blood Pressure Monitoring (ESH), the British Hypertension Society (BHS), and the International Organization for Standardization

(ISO) [61; 62; 63]. These standards differ in aspects like the size of the study population (AAMI, BHS: 85, ESH: 33) and the relative size of each blood pressure (BP) population of interest, such as hypotensive and hypertensive subjects. In a collaborative effort by standardization committees (AAMI/ESH/ISO), a new consensus document was released in 2018 (revised in 2019) in an attempt to unify the standards [59; 27]. The AAMI/ESH/ISO standard comprises a study size of 85, including a minimum number of subjects within certain BP ranges [64]. For continuous BP instruments, the suitability of these protocols, designed for spot measurement BP devices, raises questions and requires further investigation. These protocols, designed for validation of cuff-based instruments, are not generally applicable to cuffless devices, particularly those requiring calibration.

The Institute of Electrical and Electronics Engineers (IEEE) has introduced a standard protocol specifically tailored for wearable cuffless devices, IEEE 1708-2014 [65], with an amendment released in 2019 (IEEE 1708a-2019) [66]. Despite this, the standard has not yet gained widespread use. Notably, the IEEE protocol differs from standards for traditional cuff devices, requiring a noticeable change in BP to be induced and the calibration to hold for a specified period. The validation protocol comprises two phases: phase I (n = 20) and phase II ($n \geq 65$). If results from phase I meet the standard, phase II is initiated. The key difference between the phases is the number of participants enrolled. Each phase involves three sets of measurements. After the initial calibration specified by the manufacturer, the first measurement set is compared against manual auscultation. For the second set, a change in BP must be induced, which can be achieved through methods such as a cold pressor test (CPT), passive leg raising (PLR), or an exercise stress test. The third set is conducted after a predefined period to ensure the validity of the calibration. The protocol is outlined in Figure 6.

In certain cases discussed below, a modified protocol (e.g., insufficient pressure range or sample size) has been employed, rendering devices not fully validated. One device failed to meet the standard criteria and is considered inaccurate. In many instances, multiple manufacturers have adopted the same technology due to patent rights expiration or the technology being implementable through different methods. Some modern instruments cannot exclusive be categorized into a single group, as they utilize multiple technologies. For instance, the Caretaker 4 monitor uses oscillometry for initial calibration but relies on pulse wave analysis (PDA) for BP tracking [51; 52]. Examples of each technique will be introduced, and Figure 7 and Table 1 summarize the features of each device.

2.2.1 Miniaturization of cuff oscillometry

Common digital blood pressure (BP) devices used in medical offices and homes, whether at the doctor's office or nowadays even integrated into wearables, are typ-

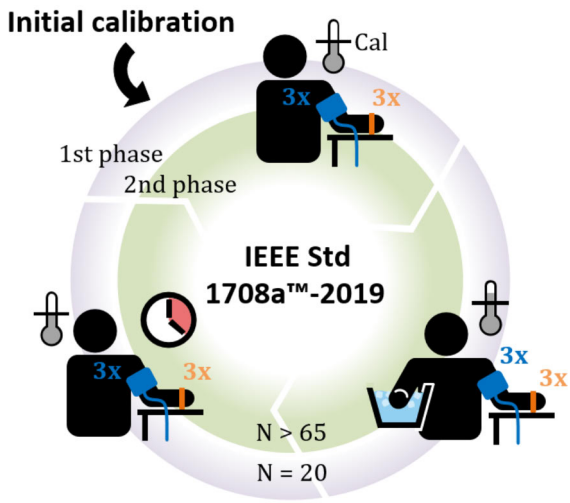

Figure 6. IEEE Standard for Wearable, Cuffless Blood Pressure Measuring Devices first introduced in 2014, amended in 2019. The protocol provides a more dependable means of evaluating the precision of continuous BP devices when compared to conventional standards. Here, a cold pressor test is employed to induce BP variations, although alternative methods conducive to the same objective may also be utilized [66]. Figure adapted from [22].

ically based on cuff oscillometry. An example is the Omron Heartguide (OMRON Corporation, Japan), a smartwatch which incorporates a miniature cuff into the watch strap [67]. Similar to traditional brachial cuff devices, users are required to sit still and initiate spot measurements. Proper placement at heart level minimizes errors introduced by the hydrostatic effect, and the device measures a basic oscillometric pressure response. The watch can be connected to a smartphone app for tracking 24-hour BP trends. Validation of the standard-size cuff (n = 85) using the AAMI protocol for non-invasive BP measurement devices yielded SBP and DBP values of (-0.9 ± 7.6) mmHg and (-1.1 ± 6.1) mmHg, respectively [67]. Although wrist cuff oscillometry has been utilized in various devices, the Heartguide stands out as the first to successfully miniaturize the cuff into a watch strap of reasonable size [68].

The Caretaker 4 (Caretaker Medical, US) is a wearable wrist-mounted monitor equipped with a small inflatable finger cuff, enabling continuous BP measurement. It relies on the oscillometric method for calibration, and its self-calibration has been validated (n = 126) according to the AAMI standard, resulting in SBP and DBP values of (-1.4 ± 6.7) mmHg and (2.2 ± 6.4) mmHg, respectively [51].

The Finger-port (Elfi-Tech, Israel) is a compact tabletop finger cuff device utilizing dynamic light scattering (DLS) technology to measure blood flow alterations in the finger during cuff deflation. This device, capable of measuring various vital signs in addition to BP, has not yet undergone validation according to any international standard protocol [69].

2.2.2 Oscillometric finger pressing method

The method of oscillometric finger pressing was conceived in 2018 [70]. In this approach, a smartphone is modified by incorporating a phone case equipped with PPG and force sensors, or alternatively, the smartphone's internal sensors can be utilized [71]. The user exerts increasing force on the sensor to simulate cuff inflation, and the accompanying app guides them on the applied pressure. The PPG sensor captures blood volume oscillations in the finger, enabling the extraction of an oscillogram from the optical signal. Simultaneously, the force sensor records the pressure ramp. Subsequent standard oscillometric analysis is performed using the combined optical and pressure signals. In the initial study (n = 32), this method demonstrated an accuracy of (3.3 ± 8.8) mmHg for SBP and (-5.6 ± 7.7) mmHg for DBP. It's noteworthy that the device was compared against an oscillometric brachial cuff device rather than the gold-standard auscultation, and the study protocol did not strictly adhere to any international standard. Nevertheless, the study illustrated the feasibility of using a smartphone for blood pressure measurement with minimal additional equipment.

A comparable technology was introduced in a US patent application by Leman Micro Devices in 2014 [72]. The developed V-sensor incorporates a PPG sensor and a pressure sensor, alongside other biosensors. Unfortunately, the operational principle and accuracy of the device have not been fully disclosed, as there are no peer-reviewed studies available [73]. The company has announced through their press release that the sensor can be integrated into a smartphone or wearable device. Similar to the approach by Chandrasekhar et al. [70], users apply pressure to the sensor while receiving feedback through the app. The company claims that the technology is validated according to the ISO standard, with reported results of (-0.4 ± 7.2) mmHg for SBP and (-0.2 ± 6.0) mmHg for DBP, respectively [73].

2.2.3 Tonometry

BPro (Healthstats, Singapore) is a wristwatch equipped with a radial artery tonometer, specifically designed for ambulatory BP measurement. The device requires an initial calibration using a brachial cuff device, and post-calibration, it is expected to provide accurate BP readings for a minimum of 24 hours. The device includes a watch head with a graphical user interface and a separate plunger module designed to be pressed against the radial artery. During calibration, healthcare professionals secure the plunger to the wrist using double-sided tape to ensure stability during use. The device has been validated according to the standards set by the American Association for the Advancement of Medical Instrumentation (AAMI) and the European Society of Hypertension (ESH), resulting in SBP and DBP values of (-0.9 ± 7.6) mmHg and (-1.1 ± 6.1) mmHg, respectively [74].

2.2.4 Pulse propagation methods

The utilization of PTT or PAT for BP estimation has been adopted by various companies, with attempts to measure absolute BP via PTT/PAT. However, it appears that this method is better suited for assessing relative changes in calibrated BP than for spot BP measurements. Consequently, PTT/PAT may be useful for ambulatory BP monitoring but requires an additional instrument for calibration.

Biobeat (Biobeat, Israel) and SOMNOtouch NIBP (SOMNOmedics GmbH, Germany) are smart wristband-based devices that employ PAT measured by ECG and wrist PPG to track BP [75; 76]. SOMNOtouch utilizes an ECG module with traditional ECG electrodes wired to the wrist device, while Biobeat uses a separate wireless and wearable ECG patch in conjunction with the wrist module. Both devices are calibrated with an oscillometric device, and assess continuous BP by measuring the pulse arrival time from the ECG R-peak to the PPG pulse in the wrist or finger. In a study comparing Biobeat to a sphygmomanometer, the device demonstrated SBP and DBP values of (-0.1 ± 3.6) mmHg and (0.0 ± 3.5) mmHg, falling within the range of the ISO 81060-2:2013 standard [76]. However, slight modifications were made to the study procedure. SOMNOtouch, validated using the ESH protocol, yielded SBP and DBP values of (-0.4 ± 6.1) mmHg and (-0.1 ± 3.6) mmHg, respectively [75]. The applicability of AAMI/ESH/ISO standards for devices based on PAT remains unclear, as these standards are designed for spot measurement devices that do not require initial calibration. In both studies, the devices were first calibrated to auscultatory BP values, and validation measurements were conducted shortly after calibration. Thus, the stability of accuracy over longer periods and during significant pressure variations remains uncertain. A recent study comparing SOMNOtouch to an ambulatory oscillometric device showed poor agreement between the two [77], suggesting that similar conditions would likely yield comparable results for Biobeat.

Freescan monitor (Maisense Inc, Taiwan) is a handheld device employing single-lead ECG and applanation tonometry to measure BP via PAT. The tonometer probe is placed on the radial artery to measure the radial pulse, and PTT is calculated from the ECG R-peak to the foot of the radial pulse. This device is suitable only for spot measurements, requiring active user actuation, and a single measurement takes approximately 10 seconds. The device relies on initial calibration, performed once for each subject, and a validation study according to AAMI/ESH/ISO standards resulted in (3.2 ± 6.7) mmHg and (2.6 ± 4.6) mmHg for SBP and DBP, respectively.

The Instant Blood Pressure app (AuraLife, US), introduced in 2014 and later discontinued, utilized pulse transit time from seismocardiography (SCG) and PPG signals for BP measurement. The app, available on digital marketplaces, was found to be highly inaccurate in a 2016 study using AAMI/ESH/ISO protocol, with SBP and DBP results of (-1.2 ± 16.2) mmHg and (7.1 ± 10.8) mmHg, respectively. This inaccuracy led to the misclassification of hypertensive patients as normotensive, po-

tentially resulting in untreated individuals. A Federal Trade Commission complaint was filed in 2016, leading to a settlement [78].

Glabella, a smart glasses prototype developed by Microsoft for continuous BP monitoring, features three PPG sensors embedded in the frame to measure PTT between the angular, superficial temporal, and occipital arteries. Similar to other PTT devices, Glabella relies on initial oscillometric calibration. Additionally, the glasses incorporate an accelerometer unit to filter out motion artifacts. Although the device's accuracy is unproven, it has undergone proof-of-concept measurements on a few individuals (n = 4) [79].

A recent method demonstrated the estimation of BP using multi-wavelength PPG signals [80]. By utilizing light at different wavelengths, the method penetrated the skin at varying depths, probing different blood vessels. Shorter wavelengths (blue, green, and yellow) focused on smaller vessels like arterioles and capillaries, while longer wavelengths (red and infrared) penetrated deeper, measuring arterial blood flow in the arteriovenous plexus. The time delays between these signals correlated with BP, and comparison between normotensive and hypertensive subjects yielded mean absolute differences against reference measurements of (2.2 ± 2.9) mmHg and (1.4 ± 1.8) mmHg for SBP and DBP, respectively [80].

2.2.5 Pulse wave morphology

The Caretaker 4 employs PDA technology for continuous monitoring of BP changes over time. After the initial BP values are measured or manually entered, the device applies a constant pressure of 40 mmHg to the finger cuff. Pulsations in the cuff are recorded and analyzed using PDA. The accuracy of continuous BP monitoring has been validated in a study with 24 participants, resulting in SBP and DBP values of (-0.4 ± 7.7) mmHg and (-0.5 ± 7.0) mmHg, respectively [52].

Valencell utilizes the PWA approach in its wireless earbud device. The earbud, traditionally used for music listening, incorporates a PPG sensor and supporting electronics. The device relies on optical pulse wave morphology analysis combined with machine learning. According to a white paper published by the company, the earbud can achieve accuracy similar to an oscillometric cuff monitor, with SBP and DBP values of (1.7 ± 7.7) mmHg and (-1.1 ± 8.0) mmHg, respectively [81].

The Aktiia bracelet is another device utilizing PWA of PPG signals. Developed by a Swiss company, this wearable wristband, similar to fitness activity bracelets, incorporates an off-the-shelf PPG sensor. Calibration with an oscillometric device is required, and the company claims that a single calibration provides accurate results for up to two months [82]. Although the study results comparing the technology to invasive BP catheter readings have not yet been peer-reviewed, the company asserts that the results fall within the range of the ISO standard, with SBP and DBP values of (5 ± 8) mmHg [82].

Pulse morphology analysis has extended to smartphones with the introduction of the OptiBP app (Biospectal, Switzerland). The app employs PPG combined with PWA to measure spot BP. Instead of a dedicated PPG unit, the app utilizes a smartphone camera and LED flash to capture the PPG waveform. The camera flash replaces a single LED with a specified wavelength, and the CMOS cell acts as an optical sensor. The system is trained using measurements from an invasive BP recording (n = 51) obtained in an operating room environment. In validation (n = 40), the device was compared against manual auscultation, resulting in SBP and DBP values of (-0.7 ± 7.7) mmHg and (-0.4 ± 4.5) mmHg, respectively. The protocol used raises questions about its validity, and consideration of a protocol similar to the IEEE 1708a-2019 standard is suggested for devices relying on individual calibration [83].

2.2.6 Transdermal optical imaging

Transdermal optical imaging (TOI) for the monitoring of BP utilizes remote PPG to capture changes in blood flow on the facial skin [84; 85]. The method involves directing light onto the skin while simultaneously using a camera to capture the light reflected from the outer layer of the skin (epidermis). The camera flash emits white light produced by three LEDs (red, green, and blue). As each wavelength penetrates different skin layers, probing various blood vessels allows for a comprehensive assessment of skin vasculature. The smartphone camera detect subtle pulsations in facial blood vessels, generating a map of 17 distinct facial sections. The measurement data is fed into a machine learning model, which outputs SBP and DBP. The model was trained on a dataset comprising 1328 measurements, with 85% used for training and 15% for validation. The study reported SBP and DBP values of (-0.5 ± 8.9) mmHg and (-0.4 ± 6.2) mmHg, respectively. However, the accuracy and precision fell short of AAMI standard requirements. Moreover, the study focused exclusively on normotensive subjects, making it challenging to extrapolate the findings to hypotensive or hypertensive cases, which are often more challenging to measure reliably. The statistical power of the dataset collected is insufficient for drawing robust conclusions, indicating the need for further validation to confirm the accuracy of TOI data in BP estimation.

2.3 Modeling and algorithms

The emergence of new computational techniques has opened new possibilities to improve BP monitoring and hypertension management. These techniques are typically based on models relating physiology with measured parameters or statistical models with recent emphasis on machine learning.

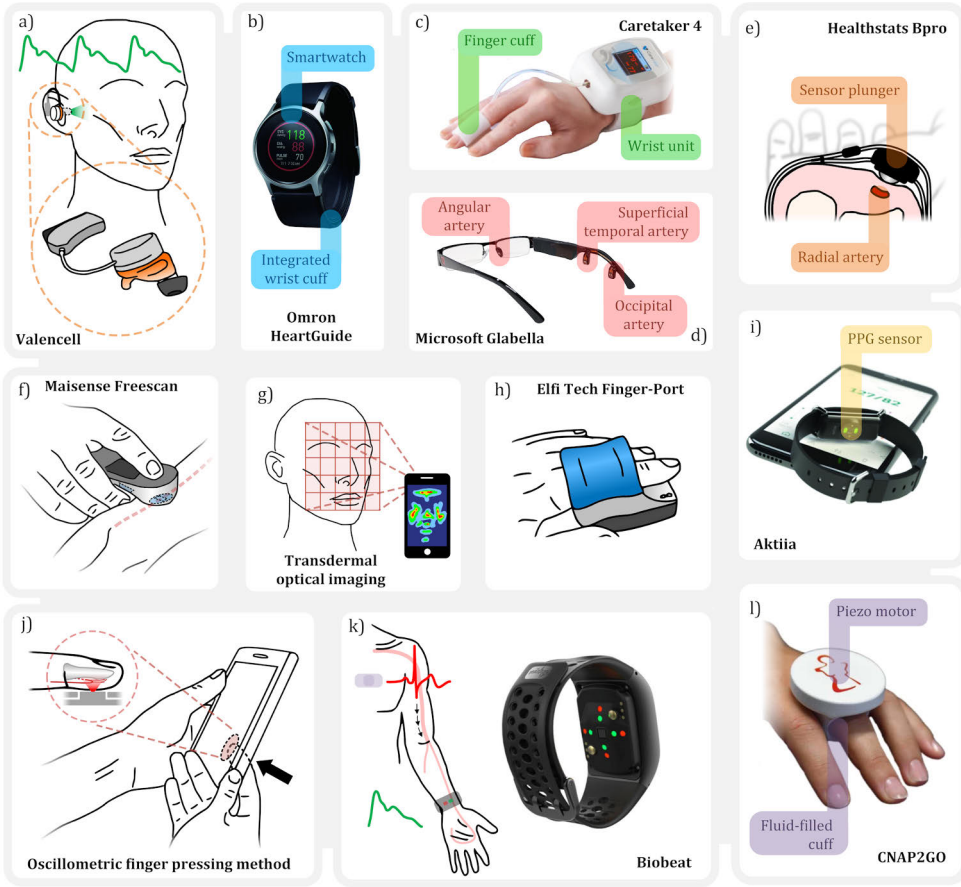

Figure 7. Collection of recent instruments. a) Valencell ear-buds use PPG waveform analysis and a machine learning model [86]. b) Omron Heartguide is a smartwatch equipped with an inflatable miniature cuff. Figure adapted from [67] c) Caretaker 4 uses a finger cuff and PDA technique to measure continuous BP. Figure adapted from [52]. d) Glabella is a smart glasses prototype developed by Microsoft, that uses multisite PPG to assess BP. Figure adapted from [79]. e) Healthstats BPro uses a smartwatch form factor and radial tonometry to measure arterial pulse continuously [74]. f) Maisense Freescan uses combined ECG and radial tonometry to measure PTT [87]. g) In transdermal optical imaging (TOI) a smartphone is used to capture remote PPG via the built-in camera. BP is computed using artificial intelligence techniques [84]. h) The Fingerport developed by Elfi-Tech uses an inflatable finger cuff along with micro dynamic light scattering (mDLS) technique to measure BP [69]. i) Aktiia is a wrist-worn bracelet that measures BP using PPG combined with pulse wave analysis (PWA). Figure adapted from [88]. j) In oscillometric finger pressing method user actuates the measurement by applying increasing pressure to the sensor mounted on the smartphone case [70]. The V-sensor developed by Leman Micro Devices uses a similar approach [73]. k) Biobeat is a smart watch type device that uses PTT to measure BP. ECG is collected with a chest patch. Figure adapted from [76]. SOMNOtouch uses a similar approach [75]. l) CNSystems CNAP2GO is a smart ring that uses volume control technique to measure continuous BP. Figure adapted from [56].

Device	Technology	Spot BP	Cuffless	Calibration	PWA	Beat-to-beat BP	Validation (n)	References
Omron Heartguide	Cuff oscillometry	Yes	No	No	No	No	AAMI (85)*	[67]
Healthstats BPro	Radial artery tonometry	No	Yes	Yes	Yes	Yes	AAMI, ESH (89)*	[74]
Elfi-Tech	Cuff oscillometry & mDLS	Yes	No	No	Yes	No	-	[69]
Caretaker 4	Cuff oscillometry & PDA	Yes	No	No	Yes	Yes	AAMI (126)*	[51; 52]
Smartphone (IBP app)	PAT	Yes	Yes	No	No	No	Failed (85)	[78]
SOMNOtouch NIBP	PAT	No	Yes	Yes	No	Yes	ESH (33)	[75]
Biobeat	PAT	No	Yes	Yes	No	Yes	ISO (1,057)*	[76]
Maisense Freescan	PAT	Yes	Yes	Yes	No	No	ISO (100)	[87]
Valencell	Ear PPG	Yes	Yes	No	No	Yes	ISO (147)	[86]
Smartphone (OptiBP app)	PPG PWA	Yes	Yes	Yes	No	No	(40)	[83]
Aktiia	PPG PWA	Yes	Yes	Yes	No	No	ISO (86)†	[82]
Microsoft Glabella	PTT	Yes	Yes	No	No	No	(4)	[79]
LMD V-sensor	Riva-Rocci & PPG	Yes	Yes	No	No	No	-	[73]
FANTOM	Tonometry & Oscillometry	Yes	Yes	No	Yes	Yes	(33)	[11]
Smartphone	Finger pressing method	Yes	Yes	No	No	No	(32)	[70]
Smartphone	TOI	Yes	Yes	No	No	No	(1,328)	[84]
UT9201	Differential oscillometry	Yes	No	No	No	Yes	(22)	[58]
CNAP2GO	VCT	Yes	No	No	No	Yes	(46)	[56]

* FDA approval, † CE mark

Table 1. A survey of the reviewed devices and technologies. The devices have been divided into two categories: commercial (top) and research (bottom) devices. Spot BP indicates whether the device can be used to take single user activated BP measurements. The calibration column indicates whether the device has to be calibrated to external arm cuff readings. PWA column indicates whether the device outputs pulse wave morphology information to the user. Validation status is disclosed by naming the used standard (if one is used) and the number of subjects in the study. A superscript shows whether the device has gained US FDA approval or European CE mark. Table adapted from [22]

2.3.1 Physiological models

The Windkessel model is a 0-dimensional, or a lumped parameter model used for describing a part within the circulation or the whole system itself [89]. It takes into account the compliance and resistance of the blood vessels, by representing these characteristics using linear circuit components. There are three ways to achieve this: a) two-element, b) three-element and c) four-element Windkessel models. In two-element model, the resistance of the vessel is modeled via a resistor (R) and the compliance is modeled using a capacitor (C), in parallel configuration. The three-element model adds another resistive element (Z_c) in series with the two previous ones, accounting for the characteristic impedance of the aorta. Finally, the four-element Windkessel model incorporates an inductor (L) to the circuit in order to account for the inertia of the blood flow. The most commonly used one of these is the three-element model, which can be represented as a differential equation:

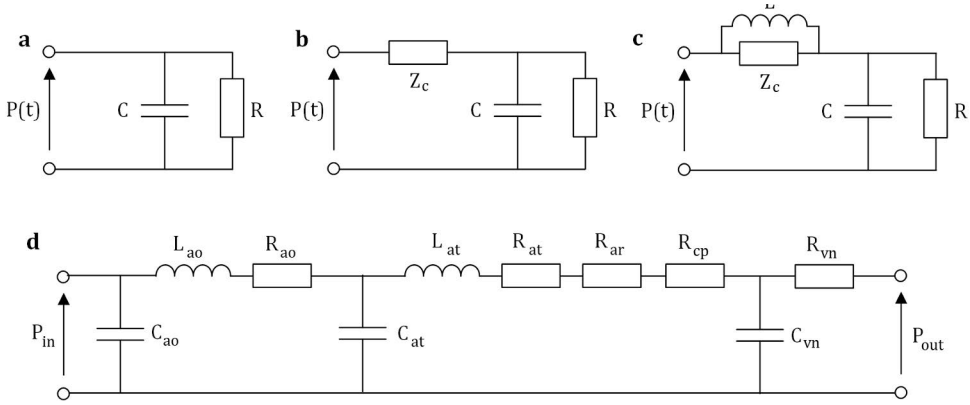

Figure 8. Windkessel model circuits. a) Two-element Windkessel model. b) Three-element Windkessel model. c) Four-element Windkessel model. d) A Multi-compartment Windkessel model representation incorporating the aorta, arteries, arterioles, capillaries and veins.

$$(1 + \frac{Z_c}{R})I(t) + CR_1\frac{dI(t)}{dt} = \frac{P(t)}{R} + C\frac{dP(t)}{dt} \tag{4}$$

where Z_c is the characteristic impedance, R is the peripheral resistance, C represents the arterial compliance, L represents the inertia of blood flow and P(t) is the pressure as a function of time t. Combining these mono-compartment models, it is possible to model a larger section of the circulation. Figure 8d depicts a multi-compartment model of the systemic circulation, including the aorta, arteries, arterioles, capillaries and finally veins. [89]

Understanding the behaviour of the pressure coupling mechanism from the artery to the cuff is important in examining the oscillometric method. A mathematical model describing this relationship has been introduced in [35]. Arterial compliance describes the relationship between the transmural pressure and the dynamic volume changes measured in the cuff. This is often depicted in a pressure-volume curve. Arterial compliance (C_a) can be expressed using a piecewise first-order differential equation:

$$C_a = \begin{cases} \frac{dV_a}{dP_t} = aV_{a0}e^{aP_t}, \text{ when } P_t < 0 \\ \frac{dV_a}{dP_t} = aV_{a0}e^{-bP_t}, \text{ when } P_t \geq 0 \end{cases} \tag{5}$$

where V_a is the arterial volume, a and b are constants describing the stiffness of the artery, and V_{a0} is the arterial volume at zero external pressure. Arterial compliance is expressed in μl/mmHg. In the study, the author created a simulated response which was compared to the model output and the one providing the smallest least squares residuals revealed the most likely BP values. The model was accurate under different simulated arterial compliances. [35]

The traditional oscillometric method, which relies on a fixed ratio based on population averages, tends to yield inaccurate blood pressure (BP) estimates due to inter-subject variability. This inaccuracy is particularly evident in oscillometry, where changes in arterial compliance can modify the shape of the pressure oscillation envelope, impacting the estimated SBP and DBP values, especially when employing fixed ratio methods [33]. To enhance accuracy, patient-specific algorithms have been developed [34; 90]. These algorithms involve fitting a parametric arterial volume-pressure model to the measured envelope of pressure oscillations, and the subsequent best-fit calculation provides more precise estimates for SBP, DBP, and parameters characterizing the volume-pressure relationship. In a different study, the Windkessel model of the arterial system, which considers total vascular resistance and compliance, was incorporated. This integration with the measured oscillometric envelope demonstrated a potential reduction in the discrepancy between oscillometric and auscultatory measurements [91].

2.3.2 Machine learning

Machine learning and artificial intelligence have recently been utilized in hemodynamic monitoring, especially in the field of continuous BP [92]. For instance, a study focused on continuous BP estimation employed multivariate linear regression (MLR) and support vector regression (SVR) models, utilizing 14 features derived from waveform morphology and time intervals from ECG and PPG data. The model, tested on 73 subjects, reportedly exhibited robust performance, maintaining efficacy when assessed 1, 3, and 6 months after its creation [93]. Another investigation utilizing similar machine learning models evaluated numerous databases with approximately a thousand subjects. Employing 10-fold cross-validation, the models achieved average deviations of 5.7, 9.9, and 5.3 mmHg for DBP, SBP, and MAP, respectively, with negligible biases [93]. In another study, a deep learning algorithm, tested on digital stethoscope recordings, demonstrated an approach to directly measure both SBP and DBP. After digitizing the recordings, image classification techniques were applied, showcasing promising proof-of-concept across 30 subjects [94]. Similarly, a machine learning approach utilizing features from PPG and ECG signals successfully differentiated normotensive from hypertensive subjects, including those with pre-hypertension [95].

A recent investigation explored the use of machine learning to estimate BP from pulse oximeter PPG signals [96]. Deep convolutional networks, analyzing 30-second PPG segments from 329 subjects, demonstrated reliable BP estimation in a hospital setting. Mean absolute errors for SBP, DBP, and MAP were reported as (0.48 ± 9.81) mmHg, (0.44 ± 5.16) mmHg, and (0.47 ± 5.63) mmHg, respectively. The study claimed that BP tracking precision remained robust with signal durations up to 600 minutes [96]. Another study explored features derived from PPG morphology as

markers for BP [97]. Analyzing waveform simplifications and subsequent assessments of blood flow velocity and acceleration, correlations with BP changes were identified.

Advancements in technology have spurred significant efforts in utilizing wearables and smartphones for BP estimation. The advantages of self-monitoring include tracking average BP over time, detecting concerning trends, and identifying abnormal circadian patterns [98]. Telemonitoring systems that communicate these measurements with clinicians hold the potential to enhance hypertension management and reduce healthcare costs [98]. For example, the Cardiogram application utilized a long short-term memory network to predict hypertension using only heart rate and step count. The data, collected from 6,115 Apple Watch users over an average of nine weeks, demonstrated reasonable prediction performance with an area under the receiver operating characteristic curve exceeding 80% [99; 100]. Presently, there are over 180 apps for BP estimation designed for telemonitoring, but only a small fraction have been developed in collaboration with medical experts, and rigorous validation evidence is scarce [98]. Importantly, there are currently no mobile apps for BP measurement that have received approval from the US Food and Drug Administration or the European Commission [98].

2.4 Summary of the literature review

This literature review examines recent advancements in blood pressure (BP) monitoring and the underlying fundamental principles. The predominant focus has been on the development of continuous and cuffless monitors, the miniaturization of cuff-based devices, and the exploration of new algorithms to enhance robustness and accuracy. The progression in BP monitoring devices is moving towards a more wearable form factor, designed to be worn over extended periods, thereby facilitating improved continuous measurements. Cuffless BP monitoring solutions primarily depend on the time delay between pulse waveforms measured at various locations and pulse morphology analysis, often coupled with machine learning techniques.

Various studies have sought to enhance the accuracy of continuous BP monitoring by incorporating mathematical models and machine learning techniques. Despite notable advancements, many of these studies have encountered limitations, including a restricted number of subjects, a narrow distribution of BP values, and the absence of standardized study protocols, which hinders direct comparisons of results. The prospect of comprehensive public databases becoming more widely accessible holds the potential for accelerated progress in this field.

Some concerns have been raised regarding the thoroughness of the validation process for cuffless devices [101], and although a standard has been proposed [65], it has not yet gained widespread use. The new standard dictates a validation of the calibration, requirement of this technology, and the ability to measure changes in the BP

after varying time from the calibration. The BP monitoring industry, understandably, is regulated and relies heavily on the established international standards.

The importance of the validation creates pressure for the manufacturers to do the validation according to a standard, even though it might not be suitable for a particular type of device. In fact, it might be easier for the device to pass the traditional standard requirements compared to a more suitable one designed for this exact type of device. As development progresses and validation becomes increasingly more stringent, continuous blood pressure monitors have the potential to evolve into widely adopted technology. However, the full advantages of truly continuous blood pressure monitoring are still to be conclusively established.

Efforts to miniaturize the BP cuff are centered around the widely adopted oscillometric technique, which is used in nearly all digital BP monitors. These devices have evolved technologically and adhere to established validation standards. They can be programmed for automatic BP measurements, enabling tasks such as diurnal rhythm monitoring. However, for beat-by-beat BP measurement, additional pulse waveform measurement is necessary. The prevailing trend is shifting towards wrist devices, and ongoing research is exploring the feasibility of finger-based BP monitoring.

3 Aims of the study

The original publications had the following aims:

I Clinical assessment of a non-invasive wearable MEMS pressure sensor array for monitoring of arterial pulse waveform, heart rate and detection of atrial fibrillation
We wanted to investigate the viability of using non-invasive pressure sensing to measure arterial pulse wave. A flexible and wearable wristband, based on microelectromechanical sensor (MEMS) elements array was developed for continuous cardiovascular health monitoring. The performance of the device in cardiovascular monitoring was investigated by comparing the arterial pressure waveform recordings to an invasive catheter recording.

II An instrument for measuring blood pressure and assessing cardiovascular health from the fingertip
In this article, our aim was to develop a new convenient way to measure BP and other hemodynamic parameters. We propose a finger artery non-invasive tono-oscillometric monitor which is an automated low-cost instrument for BP monitoring from the fingertip. We introduce a pressure sensing system that was based on a modified commercial pressure sensor. Clinical study on volunteers was performed against a commercially available arm cuff device. The results comply with the Association for the Advancement of Medical Instrumentation (AAMI) standard for non-invasive blood pressure monitors.

III Continuous Blood Pressure Monitoring using Non-Pulsatile Photoplethysmographic Components for Low-Frequency Vascular Unloading
The aim of this study was to assess the ability of finger tonometry combined with PPG to measure BP continuously. We propose a simple yet effective technique for continuous BP monitoring, called low-frequency vascular unloading. Our method is based on the finding that the non-pulsatile (DC) component of the PPG correlates with blood pressure.

IV Development and Clinical Validation of a Miniaturized Finger Probe for Bedside Hemodynamic Monitoring
Our aim was to further refine the technique introduced before and present a wearable cuffless tonometric finger probe system, that uses the oscillometric

method to measure BP. The miniaturization process enabling wearability was explained in detail. We verified the functionality of the device in a clinical trial, with multiple hemodynamic parameters in addition to BP.

V Hemodynamic Bedside Monitoring Instrument with Pressure and Optical Sensors: Validation and Modality Comparison
The aim of the article was to combine our previous efforts in hemodynamic monitoring development and use that to draw new conclusions. We combined the clinical datasets from publications II and IV and analyzed them together. In addition, we were able to compare optical and pressure sensors in the context of BP monitoring, both in healthy and arrhythmic subjects. Lastly, we applied a mathematical model to deepen our understanding in the mechanisms of BP measurement.

4 Materials and Methods

The most relevant aspects of materials and methods are presented in this chapter. More details can be found from the original publications.

4.1 Reference instruments for hemodynamic monitoring

In order to validate the designs, different types of reference instruments were used throughout the studies. Invasive BP was measured on a Carescape b40i (GE Healthcare, Finland) patient monitor with an arterial catheter connected to it. iCollect data acquisition software was used to record the data. For continuous non-invasive BP, a state-of-the-art volume clamp device CNAP 500 (CNSystems Medizintechnik, Austria) was used. Intermittent non-invasive BP was measured using Intellisense M6 (Omron Healthcare, Japan) brachial cuff device and R2 (Omron Healthcare, Japan) wrist cuff device. Carotid-to-femoral pulse wave velocity and central aortic BP were measured using SphygmoCor (AtCor Medical, Australia) device and SphygmoCor XCEL data acquisition software.

Human study (n)	Technology	Instrument	Measured parameters	Reference devices	Citation
I (31)	Wrist tonometry	I	Arterial waveform, HR, AF	GE Healthcare b40i	[10]
II (33)	Automated tono-oscillometry	II	BP, CBP, arterial waveform	Omron Intellisense M6, CNSystems CNAP 500, SphygmoCor XCEL	[11]
III (7)	Low-frequency VUT	IIIa	Continuous BP	CNSystems CNAP 500	[13]
IV (49)	Automated tono-oscillometry	IIIb	BP, PWA, AF	Auscultation, Omron R2, SphygmoCor XCEL	[15]

Table 2. Summary of the human studies conducted and the instruments used. Instrument III has two versions IIIa and IIIb with the difference being, that IIIa is equipped with an optical PPG unit and capable of continuous BP monitoring. AF = atrial fibrillation, PWA = pulse wave analysis, CBP = central blood pressure

4.2 Other equipment

Electric characterization for Instrument I was done using a precision LCR meter HP4284A (Hewlett Packard, USA) and a needle tester (Rucker & Kolls, USA) controlled by a Labview (National Instruments, USA) program. Fused Deposition Modeling (FDM) parts were 3D printed in-house using a Raise3D E2 (Raise 3D Technologies, USA) printer. SLA printing was outsourced. Printed circuit boards (PCB) for publications II-IV were designed in-house and manufactured and assembled in Shenzhen, China. The two-layer boards were manufactured using the lead-free hot air solder leveling (HASL) method.

4.3 Software and firmware

Graphical user interfaces (GUI) for using the devices were developed on Python (Instruments I, IIIa and IIIb) and MATLAB (Instrument II). Embedded firmware development was done on Arduino IDE (Instrument II) and Segger Embedded Studio (Instruments IIIa and IIIb) using C programming language. Mechanical design and finite element modeling (FEM) was done using Autodesk Inventor CAD (computer assisted design) software. Electronic design was done on Autodesk EAGLE electronic EDA (electronic design automation) software. Statistical analysis and preprocessing was done on MATLAB.

4.4 Human studies

Four separate human studies were conducted during this thesis, one for each publication (I-IV). All measurements were conducted according to the Declaration of Helsinki guidelines. The methods were performed in accordance with relevant guidelines and regulations and approved by the Ethical Committee of the Hospital District of Southwest Finland and National Supervisory Authority for Welfare and Health. Written informed consent was collected from all study subjects.

4.4.1 Human study I

Three datasets were collected to assess the performance of the developed non-invasive Instrument I. The first dataset involved 13 healthy volunteers (one female) at the University of Turku. The demographic characteristics of this group were as follows (mean, standard deviation): age (34$\pm$8 years), height (179$\pm$5 cm), weight (88$\pm$22 kg), and BMI (27$\pm$6.0 kg/m^2). All measurements in this subgroup were non-invasive and conducted using the developed Instrument I.

The second dataset comprised 18 volunteers treated at the Heart Center of Turku University Hospital, who had undergone heart surgery the previous day. Non-invasive

and invasive measurements were taken simultaneously. Due to the location of the arterial cannula, non-invasive measurements were obtained from a different wrist than the invasive waveform. The patients were in a supine position during the 10-minute recording, instructed to remain silent and still. The demographic details for this group were as follows (mean, standard deviation): height (175±9 cm), weight (86±14 kg), systolic pressure (120±15 mmHg), and diastolic pressure (70±13 mmHg).

The third dataset included seven atrial fibrillation patients admitted to the Heart Center at Turku University Hospital. The demographic characteristics for this group were as follows (mean, standard deviation): height (179±5 cm), weight (87±10 kg). Measurements in this dataset were non-invasive and conducted using Instrument I.

4.4.2 Human study II

Three datasets were obtained as part of a clinical trial aimed at investigating the performance of the developed Instrument II, focusing on BP and other hemodynamic variables, which were measured and compared with reference devices.

For the first dataset (BP), measurements were conducted on 33 volunteers (weight: μ = 77 kg [range: 48 to 117 kg]; height: μ = 176 cm [range: 161 to 194 cm]; age: μ = 32 [range: 23 to 75 years], including 8 females). Instrument II was used alongside a commercially available, validated cuff-based non-invasive blood pressure (NIBP) monitor. Subjects exhibited a BP range of DBP: 56 to 84 mmHg and SBP: 93 to 146 mmHg, with four individuals on blood pressure medication. To minimize hand temperature variations, subjects with cold fingers were asked to wear a battery-operated heated glove before the first measurement. Measurements were taken with subjects in the supine position to ensure both the finger sensor and cuff-device were at heart level. Three measurements were performed on both the reference and experimental devices, and an average was calculated. Mean arterial pressure for Instrument II was obtained from the control software, while a simple formula (MAP = $\frac{1}{2}$(SBP) + $\frac{2}{3}$(DBP)) was used to estimate MAP from SBP and DBP, as the reference device did not output a MAP value. In some cases, multiple trials were conducted to ensure correct finger position and signal quality.

In the second dataset, dynamic pressure changes recorded with Instrument II were compared against a volume clamp device (n = 3). The third dataset involved central blood pressure measurements taken on selected subjects (n = 5) using the gold standard pulse wave analysis (PWA) device and Instrument II.

4.4.3 Human study III

The aim of this study was to evaluate the performance of the proposed non-invasive continuous BP Instrument IIIa. The measurements were carried out at the University of Turku, involving repeated measurements from seven subjects (age: 26–77,

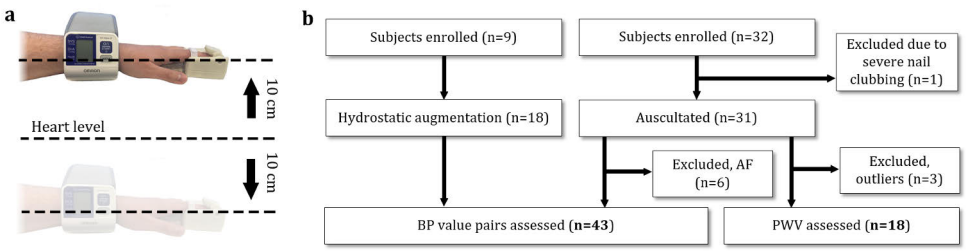

Figure 9. Human study IV. a) Hydrostatic challenge was performed on selected subjects to expand the validation dataset. b) Clinical trial flowchart. One subject was excluded due to nail clubbing which prevented reliable measurement from the fingertip. Additionally, six subjects were excluded due to atrial fibrillation. PWA was measured from 18 subjects. The final validation set was 43. Figure adapted from [15]

including three females), resulting in a total of 90 minutes of dynamic BP data. Two subjects were on BP medication. A volume clamp device served as the reference for comparison. Various BP-altering maneuvers, such as fast breathing, deep breathing, and passive leg raising, were employed to induce visible changes in BP. As not all subjects exhibited a significant response to every maneuver, we selected those with the most prominent responses. The responsivity was assessed before the actual measurements. CNAP 500 was worn on the middle and ring fingers, while our device was placed on the index finger ipsilaterally, with the subject in a supine position. Initial BP readings were obtained using the integrated brachial cuff in the reference device. Both devices were calibrated using the same BP reference values.

4.4.4 Human study IV

For the BP validation dataset, we enrolled 32 volunteers (age: μ = 47 years [range: 24 to 83 years], including 5 women) for measurements using the proposed device and manual auscultation. One subject was excluded due to severe nail clubbing. Additionally, six subjects with persistent atrial fibrillation were excluded from the BP validation dataset but were utilized to validate the detection of atrial fibrillation (AF). The validation study took place at Turku University Hospital, with subjects positioned in a supine posture to ensure alignment of both the finger device and the arm cuff at the same level. Subjects were instructed to relax and wait for 10 minutes before the first measurement to ensure stable blood pressure (BP). The finger probe was placed on the index finger, and an arm cuff connected to a mercury column sphygmomanometer was wrapped around the upper arm. Manual auscultation was performed by two trained observers, with the maximum acceptable difference between their readings set at 4 mmHg for both SBP and DBP. Following an initial test measurement, three measurements were taken in a cyclical manner, alternating between the finger device and auscultation.

To expand the BP range, we recruited an additional 9 individuals (age: μ = 48 [range: 25 to 78 years], including 4 females) to undergo a hydrostatic challenge. Four of these subjects were on BP-lowering medication. BP was measured using our device and a clinically validated wrist-worn BP cuff (Omron R2, Japan). Both instruments were worn on the same arm, positioned 10 cm below and above heart level, resulting in a total of 18 data points for SBP, mean arterial pressure (MAP), and DBP. This procedure induced a change of approximately 15 mmHg between the two levels. Three consecutive measurements were taken for both hydrostatic levels. In summary, we obtained 43 usable BP data pairs for analysis. From the initial set of 32 measurements, 6 were excluded due to AF, and 1 was excluded due to finger clubbing. To augment the dataset, we recruited an additional 9 healthy subjects who underwent the hydrostatic augmentation procedure, resulting in 18 new BP pairs. In total, this yielded 25 + 18 = 43 BP entries. In addition, we took a series of subsequent measurements to study the device's capability to take repeated measurements. The study was performed on one subject over approximately 20 minutes while comparing our device to a continuous reference. We used a volume clamp device CNAP 500 (CNSystems, Austria) as a reference. CNAP 500 is capable of outputting continuous BP data including SBP, MAP and DBP as well as the full cardiac waveform. The reference device's cuffs were placed on the middle and ring fingers ipsilaterally and our device was placed on the index finger. The reference device was calibrated using the built-in brachial sphygmomanometer at the beginning of the measurement and again at 15 minutes. A total of nine measurements were taken with our device, approximately once every two minutes. As the oscillometric sweep takes approximately 20 s, the reference BP values were averaged over 20 s for each measurement. We computed ((Mean $\pm$ SD) mmHg) for the measurements.

PWV was recorded from 18 subjects using a PWA device. The patients remained in supine position while a femoral artery cuff was wrapped around the thigh. A pen-like tonometer was used to acquire the carotid waveform. The distance between the cuff and the carotid artery via jugular notch was measured and used to calculate the PWV. An average of three consecutive measurements was used for data analysis.

5 Summary of the results

This section summarizes the results found on the four publications of this thesis. While working on Publication I, we found the fingertip to be the most suitable site for pulse wave recording, since the site is less prone to misplacement of the probe. The results from publication I aspired a shift in focus from wearable pressure sensing into automated tonometry and oscillometry as well as bedside BP monitoring in publications II-IV. Additionally, preliminary trials from publication I suggested that the fingertip is indeed the more ideal location for pressure sensing.

5.1 Wearable pressure sensing array

Instrument I was developed by Murata Electronics Oy. The system consisted of a data acquisition unit ans a wrist-strap device with three modified pressure sensors. Each pressure sensor was covered with a convex silicone layer to allow pressure transfer from the skin to the sensing element.

5.1.1 Electrical characterization

The MEMS sensor is a capacitive pressure sensor, with the top membrane and the bottom substrate acting as the capacitor plates. External pressure deforms the thin membrane, changing the distance between the membrane and the substrate, resulting in a change in capacitance. This is depicted in Figure 10a. In the actual use case, the sensors are measured with a capacitance-to-digital application-specific integrated circuit (ASIC). We used a precision LCR meter equipped with a needle tester probe setup to measure the capacitive characteristics of the sensor element.

First, the capacitive properties of the modified sensor over a frequency range were examined and compared with an unmodified element. In Figure 11a The solid lines present an average of three measurements and dashed lines show the standard deviation. The variation between different patches of pristine sensors is clearly larger than the negligible difference measured before and after the applying the silicone. It is also apparent that the sensor provides a constant capacitance value of 10.4 pF in the frequency range or approximately 1 kHz – 1 MHz in atmospheric pressure.

The pressure response of the sensor was tested by placing several weights on top of the element with the silicone bulb applied. The sensor's capacitance value follows

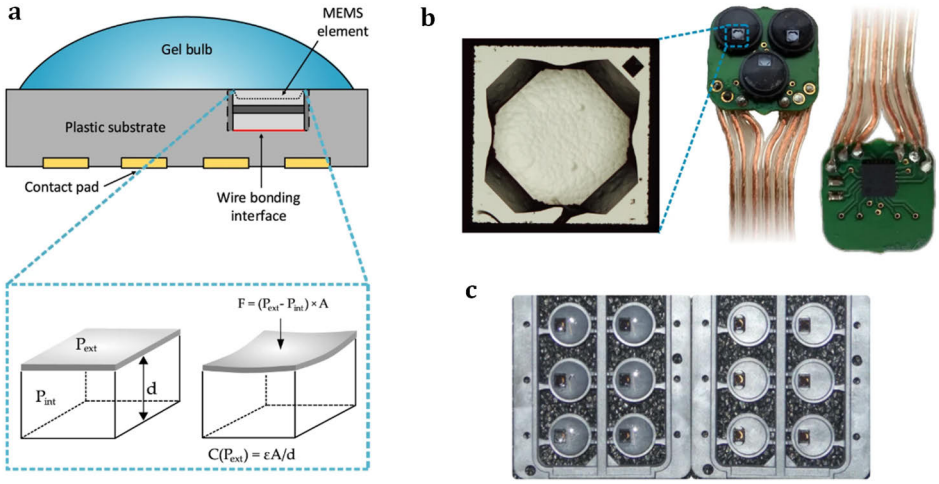

Figure 10. Sensor description for Instrument I. a) The sensor MEMS element is embedded in a plastic substrate with the element I/O pads wire bonded to the contact pads (top). The pressure sensor works by measuring the capacitance between the top diaphraghm and the base of the sensor (bottom). External pressure deforms the diaphragm, effectively shortening the distance between the capacitor plates. b) A microphotograph of the MEMS element (left) and a PCB housing three sensors. c) The sensors before and after the application of a heat-curable gel. Figure adapted from [10]

a parabolic curve at increasing weights. The response curve was fitted with a second-order polynomial resulting in a perfect R-squared value indicating good pressure reproducibility between different weights. This also suggests that the modification does not weaken the element's properties. An average sensitivity of 0.404 pF/g was achieved when using weights in the range 2–3 g and assuming a linear response.

Sensor resolution was investigated by placing a minuscule weight on the sensor. As small as a 10 mg weight creates a clearly detectable signal. This is further illustrated in Figure 11b, where the averaged values of loading and unloading with different small weights are shown. Three load/unload cycles over three different sensor elements were averaged for each weight (10, 20, 56 mg). The results seen in Figure 11 suggest that the differences caused by the loading/unloading cycle are easily observable. In addition, it is apparent that measurements can be made in absolute terms down to 10 mg.

The frequency response of the modified sensor was examined by subjecting the sensor to a fast spike-like impulse. The frequency response was then computed using fast Fourier transform (FFT). Before taking the FFT, the signal was up-sampled to 1000 Hz. The 3 dB point is found around 210 Hz. The results clearly indicate that the sensor has sufficient bandwidth for the intended application area.

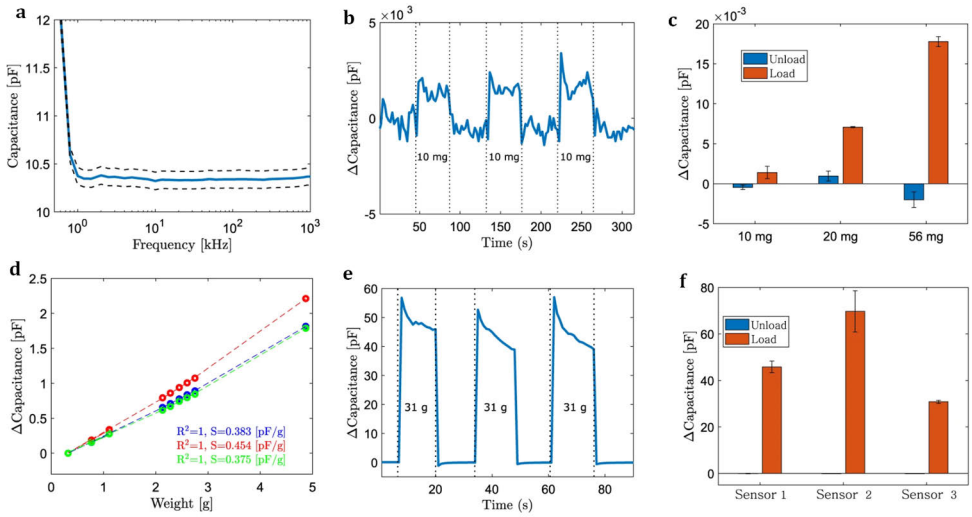

Figure 11. Sensor characterization results taken with a precision LCR meter. a) Frequency response of the sensor. b) A small weight of 10 mg was repeatedly placed on and removed from the sensor. The response is clearly visible. c) Load/unload cycles of 10 mg, 20 mg and 56 mg weights. d) An increasing amount of weights placed on the sensor showing linear response. Each color represents a different sensor. e) A large weight of 31 g was repeatedly placed on and removed from the sensor. Some hysteresis is visible possibly due to deformation of the gel material. f) Load/unload response from three different sensors. Figure adapted from [**?**]

5.1.2 Comparison to invasive arterial waveform

Non-invasive arterial pulse wave was measured using the developed instrument. Details of the study protocol and subjects can be found in Chapter 4 Materials and methods. Our aim was to assess the origin and the clinical relevance of the recorded arterial waveform and compare it with the corresponding invasive arterial pressure recording. The non-invasive the pressure reading is a sum of three components: atmospheric pressure, sensor contact pressure (the pressure that the attachment exerts on the sensor), and the physiological pressure signal caused by the expanding artery. Because the contact pressure here was not standardized the coupling of the arterial pulse to the sensor element varies between measurements. For this reason we concentrate on waveform morphology rather than the absolute pressure values.

From the ensemble averaged pulse waveforms, cross-correlation was computed between the non-invasive measurements and corresponding invasive waveforms. The averaged pulses were aligned from the systolic peaks. Figure 12 illustrates the measurement setup and typical waveforms obtained from the invasive and non-invasive recordings, and waveform shape comparison where presents both the highest, and the lowest similarity between the invasive and non-invasive waveforms in the dataset. The average Pearson correlation over all waveforms was 0.97 ± 0.02 (mean$\pm$SD) indicating high similarity between all study subjects. The difference is likely caused

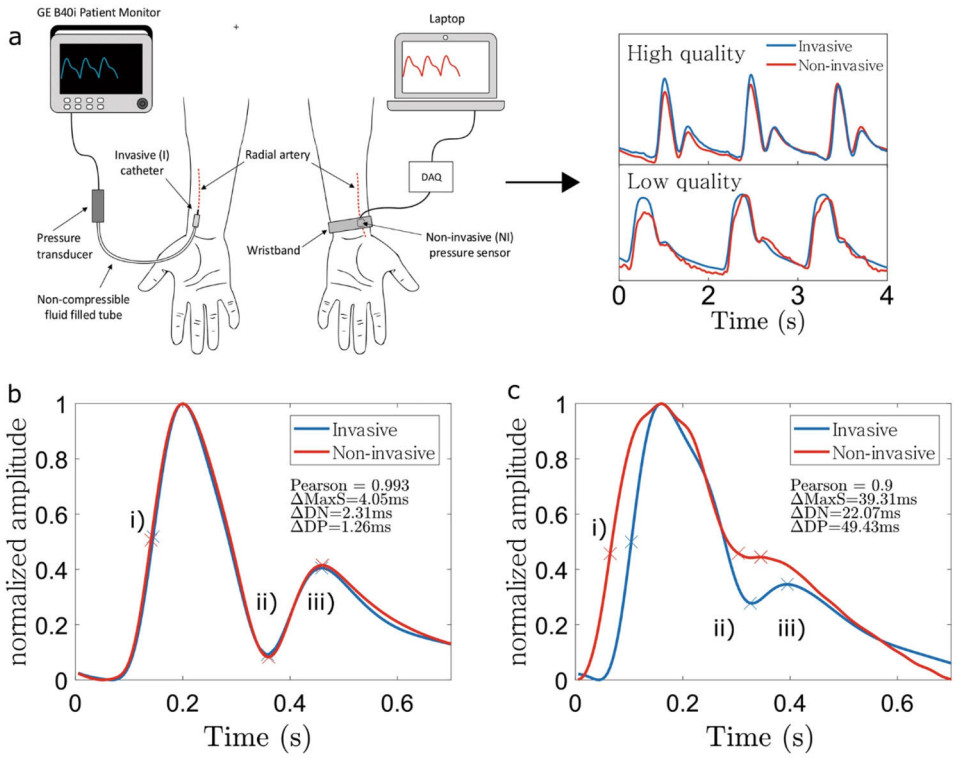

Figure 12. Clinical study results. a) An illustration of the used setup. Invasive and non-invasive signals were collected from contra-lateral hands. b) An example of a signal with high Pearson correlation of 0.99. Three fiducial points i-iii were recorded from each signal. c) An example of a signal with poor Pearson correlation of 0.9. Figure adapted from [**?**]

by the different transmural pressures across the measurements. Such high correlation has not been found with PPG signals which might be explained by the fact that PPG does not directly measure pressure waveforms, but mostly arterial blood volume variations.

5.1.3 Atrial fibrillation

Atrial fibrillation (AF) is a condition that causes the atria of the heart to contract chaotically leading to irregular heart beat. Additionally this causes large beat-to-beat blood pressure variability. These phenomena can be seen in Figure 13 where typical pressure sensor signals of a patient with AF and a healthy subject are shown. We demonstrate the ability to discriminate between sinus rhythm and AF patients (n=7) using time–frequency analysis. The classification algorithm is based on k-means clustering with two features: area under autocorrelation (AUA) and spectral entropy. The typical time traces of patients with sinus rhythm and AF are shown in

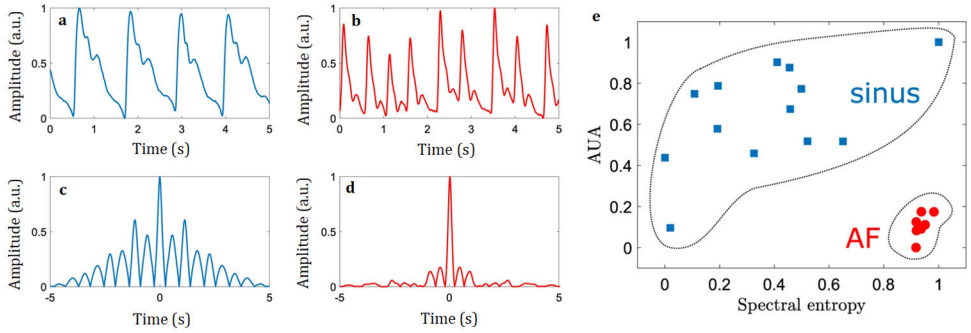

Figure 13. Atrial fibrillation detection. a) and b) Signals recorded with Instrument I from a patient with sinus rhythm and atrial fibrillation respectively. c) and d) Autocorrelation graphs computed from a) and b) respectively. e) Classification of sinus and atrial fibrillation cases based on two measures: area under autocorrelation (AUA) and Spectral entropy. Figure adapted from [**?**]

Figure 13. Both signals are clearly distinguishable and the AF shows, as expected, a higher order of irregularity between the heart beats. This is also evident in Figure 13c and d, showing the absolute value of autocorrelation function for each signal. The AF autocorrelation signal does not have clear prominent peaks outside zero lag indicating that the rhythm is irregular. In the sinus rhythm case, the peaks are clearly visible indicating regular heart rhythm. Finally, in Figure 13, the results from k-means clustering is shown. All subjects here are correctly assigned a correct cluster. It is notable that the patients with AF are all tightly clustered whereas the sinus rhythm subjects are distributed more widely. In both features, at least one healthy subject has a value similar to the AF patients indicating the need for several features for reliable discrimination. As expected, autocorrelation-based values are lower and spectral entropy values are higher on average than the respective values with healthy subjects.

5.2 Automated tono-oscillometry

The term tono-oscillometry is coined from two separate techniques: tonometry and oscillometry. In traditional tonometry the instrument is operated manually, while in tono-oscillometry the actuation is automatic and the measurement is performed during increasing/decreasing contact pressure. In regards to traditional oscillometry, the tono-oscillometric method does not use an inflatable cuff. Instead a tonometric probe and a finger pressing mechanic are used.

5.2.1 Sensing principle

The proposed technology relies on a custom-built tonometric sensor setup. The measurement process involves placing the fingertip on a piston and applying force to the

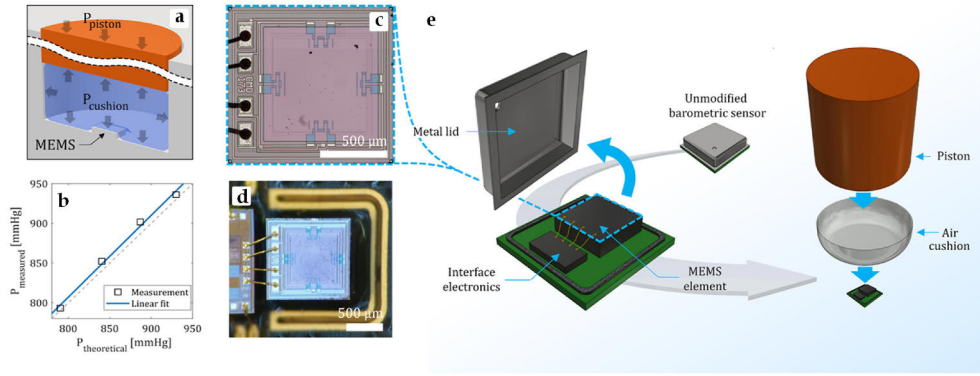

Figure 14. a) Principle of pressure coupling between the sensor and the piston surface. The pressure applied at the piston surface P_{ext} creates is balanced by an equal pressure P_{cushion} from the air cushion. According to Pascal's law, the pressure at the sensor surface is also $P_{\text{piston}} = P_{\text{cushion}}$. b) A microphotograph depicting the exposed MEMS element. c) The response of the sensor system exhibits linearity within the measured range (approximately 30 to 180 mmHg, with the measured atmospheric pressure subtracted). d) Microphotograph of a used (approximately 300 measurements) sensor element showing slight pitting on the surface. e) A barometric sensor is modified by removing the metal cover. An air cushion followed by a piston is placed on top of the sensor element. Figure adapted from [11]. Copyright 2020 Elsevier.

finger through a miniature linear motion actuator.

Pressure is defined as a force applied on an area $P = F/A$. The pressure seen at the piston P_{piston} can be expressed as a combination of two separate components P_{aeff} and P_{ext}: $P_{\text{piston}} = P_{\text{aeff}} + P_{\text{ext}}$, where P_{aeff} is the effective pressure oscillation caused by the arterial pulsation depicted as P_a. P_{ext} is the external contact pressure produced by the motion actuator and applied to the finger. The pulse pressure sensed at the sensor is attenuated due to the small diameter of the artery. The force F_a, generated by the pulsating applanated artery, remains relatively small since the contact area with the piston surface (A_{piston}) is significantly larger than the area of the small artery (A_a). The actual amplitude of the oscillating pressure, P_{aeff}, fluctuates in relation to P_{ext}, as outlined by the arterial compliance model [35]. The pressure at the fingertip surface is equivalent to the pressure P_{piston}, which, in turn, matches the pressure within the air cushion, P_{cushion}:

$$P_{\text{piston}} = P_{\text{ext}} + P_{\text{aeff}} = P_{\text{cushion}} \iff \frac{F_{\text{piston}}}{A_{\text{piston}}} = \frac{F_{\text{cushion}}}{A_{\text{cushion}}} \tag{6}$$

where F_{piston} and F_{cushion} are the forces exerted on the finger and the cushion, respectively, and A_{piston} and A_{cushion} are the corresponding areas. As the areas on top of the piston and the air cushion are nearly equal, the forces on both sides of the cushion wall are balanced. The fixed walls and floor of the cylinder prevent the cushion from expanding under external pressure. According to Pascal's law, the pressure applied to the fluid is uniformly distributed throughout the fluid. Consequently, the

pressure sensed by the MEMS sensor equals the pressure applied to the finger, denoted as P_{piston}. The morphology of the recorded arterial waveform is contingent on the prevailing transmural pressure P_t, defined as the difference between the pressure in the artery (P_a) and the applied pressure (P_{piston}), represented as $P_t = P_a - P_{\text{piston}}$. The validity of the applied pressure coupling to the sensing element can be verified by placing known weights on top of the sensor and comparing measured pressure values to those obtained by:

$$P_{\text{cushion}} = \frac{F_{\text{piston}}}{A_{\text{piston}}} = \frac{m \cdot g}{A_{\text{piston}}} \tag{7}$$

where m is the weight and g is Earth's gravity (in m/s^2). The sensor's response aligns well with the predicted values, exhibiting a linear response as depicted in Figure 14b.

5.2.2 Algorithm

From the raw pressure signal, a bell-shaped oscillogram envelope (OMWE) is constructed by equiripple bandpass filtering (1 - 10 Hz), Hilbert transform, peak detection, and polynomial fitting respectively. Since the oscillogram is asymmetric, the Hilbert transform is useful for computing OMWE, performing similar to using both upper and lower oscillogram envelopes. MAP is found at the corresponding pressure where OMWE reaches its maximum. DBP is computed by finding a point in the P_{ext} curve where the oscillogram envelope reaches 70% from the maximum value. Systolic pressure is computed from MAP and DBP values using the following formula:

$$SBP = \frac{\text{MAP} - (1-k) \cdot \text{DBP}}{k} \tag{8}$$

where k is a constant defining the ratio of BP values. Empirically, k is set to 0.3. To regulate the applied pressure in tonometric waveform recording, the maximum of the envelope serves as a reference point. The device releases pressure until it reaches the level where the envelope is at 50% of the maximum on the systolic side, ensuring that the waveform is recorded under negative transmural pressure. Arterial pulse waveform is recorded for approximately 15 seconds. A low-pass filter ($f_{\text{cutoff}} = 10$ Hz) is applied, each pulse is found using peak detection, and finally, an average peripheral arterial pulse is extracted by ensemble averaging. The arterial pulse waveform can the be used for morphology analysis.

In publication IV we used two different algorithms for computing SBP from MAP and DBP. The first algorithm implements the same method as above, using a constant k (here $k = 0.4$) for all subjects. For the second, patient-specific approach, we incorporated the arterial stiffness index (ASI) as an additional parameter in the formula for k: $k = 0.4 + l$, where $l = 5(\tilde{x}_{ASI} - ASI)$. Here, $\tilde{x}_{ASI} = 0.03$ represents

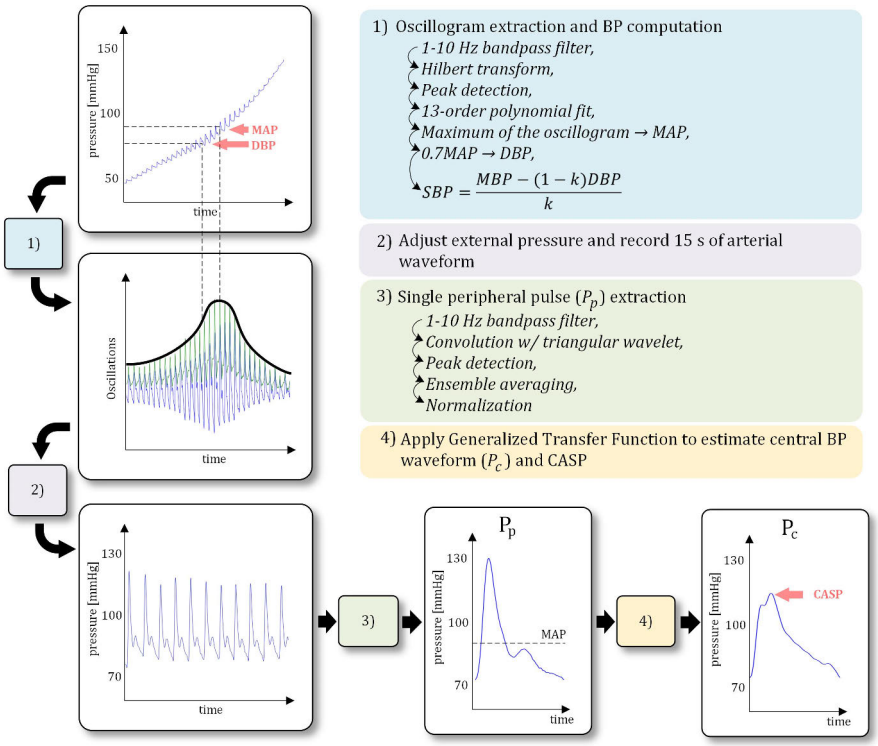

Figure 15. An algorithm for computing BP. Increasing pressure ramp is exerted to the finger generating a pressure-time plot. An oscillogram is formulated through a series of steps including high-pass filtering, Hilbert transform, peak detection, and polynomial fitting. The highest point on the oscillogram represents the MAP, and DBP is determined by identifying the point matching 70% of MAP on the left side of the oscillogram. SBP is subsequently calculated from DBP and MAP using a constant k. The pressure is then adjusted, and the arterial pulse wave is recorded for 15 seconds. A single pulse is extracted through ensemble averaging. The aortic pulse wave is constructed using a Generalized Transfer Function (GTF). Figure adapted from [11]. Copyright 2020 Elsevier.

the median of the calculated ASIs in the subject group (n = 18) with measured pulse wave velocity (PWV).

Arterial stiffness was determined by analyzing the OMWE. The OMWE was plotted against P_t. The signal underwent numerical integration, resulting in an S-shaped volume-transmural pressure (V-P_t) plot. To model the data descriptively, we employed nonlinear regression:

$$y \sim f(x, \beta)$$

Here, x is an independent variable, y is its associated dependent variable, and β is a vector of parameters for a nonlinear function f. The measured volume-pressure data was fitted to an inverse trigonometric function:

$$f(x) = \beta_1 \arctan(\beta_2 + \beta_3 x) + \beta_4$$

The parameters $\beta_{1...4}$ were computed using nonlinear fitting, and the variable x represents P_t. As β_2 describes the slope of the curve, it is used as ASI [102].

5.2.3 System design

The same sensor setup was used in both Instrument II and IIIb. The sensor is constructed using an off-the-shelf barometric MEMS pressure sensor BMP180 (Bosch Sensortec, Germany) which was customized by removing the metal packaging and placing an air-filled cushion on top of it. A plastic cylindrical piston with a diameter of 9 mm was placed on top of the cushion. BMP180 consists of a digital logic interface IC and a rectangular piezoresistive sensor chip bonded together with four gold wires. The sensor is produced utilizing Bosch's advanced porous silicon membrane (APSM) process [103]. The pressure directed to the sensor diaphragm creates deformation of the four piezoresistors on the sensor surface. Together the resistors form a full Wheatstone bridge resulting in a measurable voltage fluctuation as described in Figure 1c. The output voltage V_{out} is determined by:

$$V_{\text{out}} = \frac{1}{4R}(-\Delta R_1 + \Delta R_2 - \Delta R_3 + \Delta R_4) \cdot V_{\text{in}} \tag{9}$$

Where ΔR_1 to ΔR_4 represent changes in the resistances of the piezoelectric resistors due to tensile stress, R is the resistance of each individual piezoresistor ($R = R_1 = R_2 = R_3 = R_4$) at unloaded conditions, and V_{in} is the applied input voltage [104]. The piezoresistors are positioned at the edge of the sensor diaphragm, as the tensile stress due to diaphragm deformation is at its highest in that location. [105].

Instrument II

The electronics were constructed around the Arduino microcontroller platform, which uses the ATMega328P, an 8-bit Microchip AVR MCU (Microcontroller Unit). An extension shield was devised to interface the peripherals with the MCU board. A unipolar stepper motor (28-BYJ48, generic) and a Darlington transistor array driver (ULN2003A) are linked to a distinct motor controller MCU (Microchip AVR ATtiny84), which operates on a separate dedicated firmware. A universal asynchronous receiver transmitter (UART) connection links the motor controller MCU to the main MCU. The customized pressure sensor, situated on a separate sensor PCB, is connected to the MCU via I^2C bus. The structural components were manufactured using Selective Laser Sintering (SLS) technology to house the electronics, sensors, and the stepper motor. For the linear motion press, used to apply controlled pressure on the

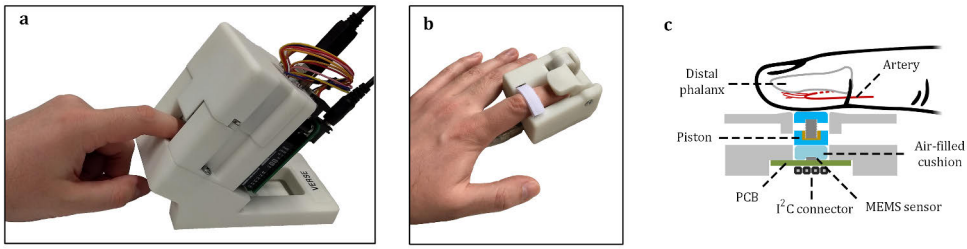

Figure 16. The developed instruments. a) Instrument II was designed to be a table-top device with the user inserting their finger into the opening in front. b) Instrument IIIb uses essentially the same technology, but in a miniaturized wearable form factor. c) Both devices use a tonometric piston construction, with an air-cushion placed on top of the MEMS element, followed by a piston. The finger is placed on top of the sensing piston while external pressure is applied to it. Figure adapted from [11; 15]

finger, a threaded rod and a nut fixed to the moving press are used to convert the motor's rotating motion into linear motion. Two brass rails were employed to stabilize the press.

Instrument IIIb

The device uses the nRF52840 (Nordic Semiconductor, Norway) microcontroller unit (MCU). The MCU was selected because of its high performance ARM Cortex M4 core and built-in USB capabilities. A pressure sensor, which is the same used in Instrument II, BMP180, is connected to the MCU via via I^2C bus. A brushed DC motor (N20, generic) is used to apply pressure to the finger. The MCU is interfaced to the motor via DRV8837 motor driver (Texas Instruments, USA) H-bridge that enables bidirectional motor control. The MCU also monitors the two limit switches (SSCQ110100, Alps Alpine, Japan) located on a separate PCB. The MCU is connected to a laptop computer via USB.

The mechanical components of the instrument hold the electronic elements, serving as a framework to generate controlled pressure to the finger and providing structural support for the tonometric pressure sensor. The enclosure was 3D printed using SLS process. A DC motor coupled with a reduction gear train is placed within the internal support enclosure. A worm gear assembly further decreases the rotational speed of the motor while changing the angle of rotation. The entire transmission mechanism is enclosed within an inner support structure. A folding press system, with the section in contact with the finger made from a flexible 3D printing filament, is utilized to exert pressure on the finger. To prevent any undesired movement and potential injuries from excessive pressure, limit switches are integrated into the hinge, establishing both lower and upper boundaries for its motion.

	SBP	DBP	MAP
Trial II	-0.9 ± 7.3	-3.3 ± 6.6	-4.3 ± 5.3
Trial IV	-3.5 ± 8.4	-4.0 ± 4.4	-1.2 ± 3.9
Combined	-1.7 ± 8.2	-0.9 ± 6.5	1.1 ± 5.3

Table 3. Summary of BP measurement accuracy of the finger probe on two separate clinical validation trials. The results are expressed as (mean±SD) mmHg

5.2.4 Validation

The tono-oscillometric technology was validated in two separate clinical studies II and IV. This section summarizes the results combined from both studies.

Blood pressure

SBP, DBP and MAP were calculated from both studies and are summarized in Table 3. Bland-Altman plots [106] including measurements taken from clinical dataset II and IV (including auscultation and the hydrostatic challenge) are shown in Figure 17. Study II (n=33) resulted in SBP, DBP and MAP of (-0.9 ± 7.3) mmHg, (-3.3 ± 6.6) mmHg and (-4.3 ± 5.3) mmHg respectively. These results comply with the AAMI/ISO standard of (5 ± 8) mmHg. However, the study size for the standard is n=85 and we opted to use the study size from the ESH standard. Moreover, the reference method used was automated cuff oscillometry, which can not be used in either of the standards.

Clinical study IV yielded results of (-3.5 ± 8.4) mmHg (-4.0 ± 4.4) mmHg (-1.2 ± 3.9) mmHg for SBP, DBP and MAP, respectively. We were able to recruit 32 volunteers in the hospital to measure with manual auscultation. However, six of them had to be excluded due to AF. With the hydrostatic challenge, the augmented dataset resulted in n=43. While DBP and MAP were well withing the limits of the AAMI/ISO standard, standard deviation in SBP exceeded the limit by 0.4 mmHg. However, the results could be improved via good algorithm design. Of the two algorithms used for computing SBP, the patient-specific method utilizing ASI, yielded better results. The standard method resulted in SBP of (-4.9 ± 9.5), which was noticeably worse than the patient-specific method. This suggests that there is indeed BP information in the ASI.

Central blood pressure

Central blood pressure (CBP) is the prevailing pressure in the aorta, representing the work the heart has to do to pump blood to the systemic circulation. Normally, CBP is lower than brachial arterial pressure due to arterial pressure amplification.

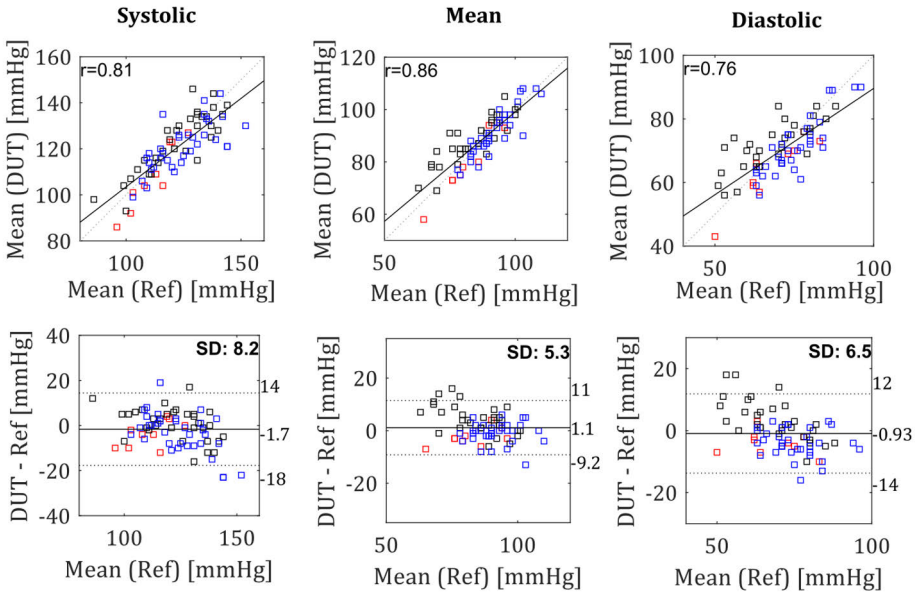

Figure 17. Correlation and Bland-Altman plots for two independent clinical trials. Datapoints from clinical trials II (white) and IV (red) and dataset IV HC (blue) are pooled into one set (n = 76). The correlation coefficient (r) and standard deviation (SD) are embedded in the figure. Figure adapted from [107]

The amplification is reduced when arteries stiffen with age and atherosclerosis, and it can vary significantly between individuals. Consequently, two individuals with the similar brachial blood pressures can have significantly different central blood pressures, with one being normotensive and the other hypertensive, requiring blood pressure medication.

One important metric is the central augmentation index ($cAIx$) [24]. The higher the $cAIx$, the more resistance the pulse wave confronts when traveling through the artery. The amplification of the reflected wave takes place as a result of diverse physiological processes, particularly when plaque begins to accumulate in the vessels (atherosclerosis), leading to a decreased ability of the vascular system to respond to both static and dynamic pressure changes. $cAIx$ can be calculated from the pulse pressures at points P_1 and P_2:

$$cAIx = \frac{PP_2}{PP_1} \cdot 100\% \quad (4)$$

where PP_1 is the pulse pressure of the initial wave, and PP_2 is the pulse pressure with the reflected wave augmented to the initial wave. The difference $PP_2 - PP_1$ is called augmentation pressure (AP).

We assessed the capability of Instrument II to measure CBP using automatically

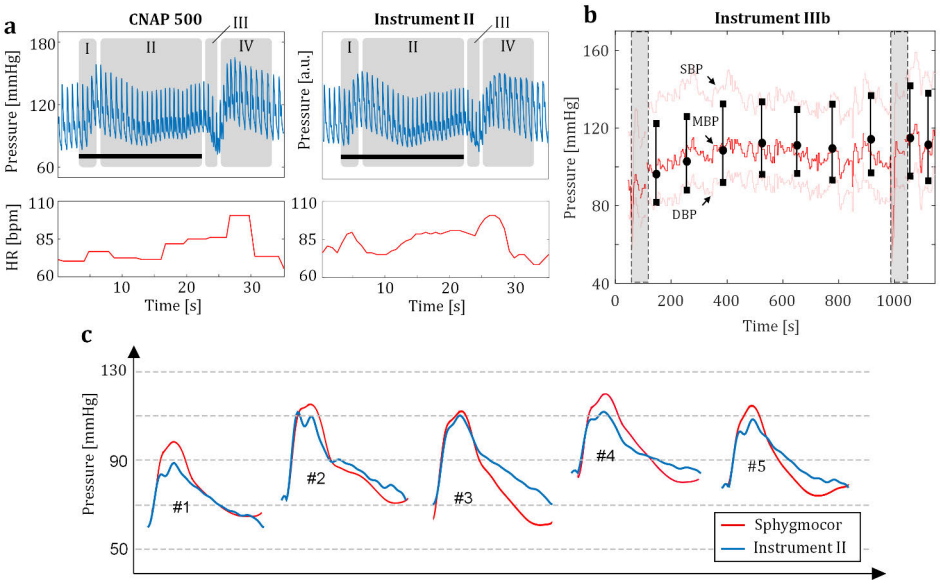

Figure 18. BP and CBP waveform recordings. a) Pressure and heart rate measured during Valsalva maneuver (indicated by the horizontal black bar) measured with Instrument II and the reference VUT device from contralateral hands. Each phase of the response is denoted as I-IV. b) Subsequent measurements taken with Instrument IIIb with a VUT device as a reference. The grey rectangles indicate automatic calibration sequences performed by the reference device. c) Five CBP pulses taken with Instrument II and the PWA reference device. Figure adapted from [11; 15]

acquired peripheral arterial waveform. A transfer function was used to estimate the CBP waveform from a peripheral pulse wave [108]. Figure 18 shows the measurements taken from five subjects with SphygmoCor and Instrument II. Comparing these two devices, central aortic systolic pressure (CASP) and $cAIx$ obtained from the CBP waveform resulted in -5.8 ± 3.2 mmHg and $1.4 \pm 6.2\%$, respectively.

Pulse wave recording

To assess the sensor's capability in capturing dynamic blood pressure changes, a Valsalva maneuver was performed on three subjects, with simultaneous measurements taken using both the reference device and Instrument II. The Valsalva maneuver is a standard diagnostic procedure, which involves the subject attempting to exhale against a closed airway [109]. The typical Valsalva response comprises four distinct phases (I to IV). In phase I, as intrathoracic pressure (ITP) increases, there is a flow of blood from the pulmonary circulation into the left atrium, resulting in an initial rise in pressure and heart rate (HR). In phase II, the increased ITP leads to a reduction in pressure and stroke volume, prompting compensatory tachycardia and a further increase in HR. With the conclusion of the maneuver in phase III, a rapid

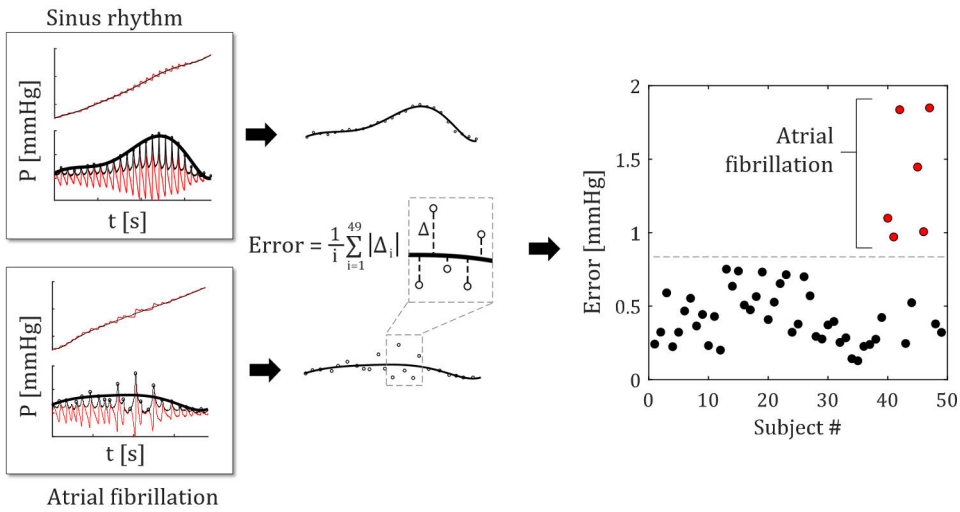

Figure 19. An illustration of AF detection during oscillometric measurement. Comparison of an envelope error feature between AF (n=6) and SR (n=43) for pressure sensor. Figure adapted from [13]. Copyright 2020 Elsevier.

pressure decrease is typically observed. This is followed by phase IV, characterized by a pressure increase surpassing the initial level and a decrease in HR. As illustrated in Figure 18a, the response recorded with Instrument II closely aligns with the reference measurement.

We aimed to evaluate the device's ability to perform successive measurements with Instrument IIIb. Nine consecutive measurements were obtained from the same subject over a 20-minute period. The consecutive measurements captured with our device closely aligned with those from the reference device, faithfully reflecting the changes in blood pressure. Comparison of the repeated measurements to the reference device resulted in SBP of (6.9 ± 4.7) mmHg, MBP of (0.6 ± 4.0) mmHg, and DBP of (1.6 ± 3.4) mmHg. The entire measurement is shown in Figure 18b.

Atrial fibrillation

We aimed to demonstrate the device's ability to detect AF while simultaneously being able to exclude these patients from the actual validation dataset. AF is known to significantly impact oscillometric blood pressure (BP) measurements. AF was identified in six subjects, and the mean error from the OMWE in mmHg was computed for each subject. In AF, pulse pressure varies randomly, causing deformation of the oscillometric envelope. Single pulses may be higher or lower than the OMWE, leading to an increase in the mean error. A threshold of 0.8 mmHg was employed to distinguish AF from sinus rhythm. Figure 19 illustrates that AF cases can be classified using this simple threshold.

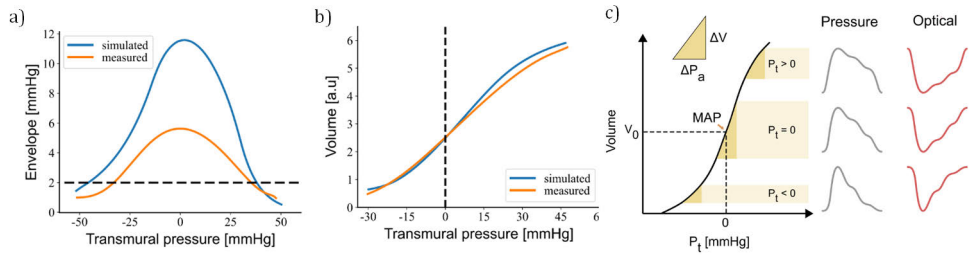

Figure 20. Oscillometric model. a) The simulated and measured OMWEs from the fingertip. b) A $V - P_t$ plot computed from a). c) The principle of the transfer of pulsations from the artery to the air cushion at different transmural pressures. Figure adapted from [107]

5.2.5 Modeling

The mechanism of pressure transfer from the artery to the cuff has been well documented in brachial oscillometry [35]. We applied the pressure-volume model described in Chapter 2, Section 3.1, to the finger tono-oscillometric method. Instead of the parameters used for the brachial artery and a brachial cuff, we used the dimensions of the air cushion and the distal transverse palmar artery [110]. This resulted in an OMWE with the maximum amplitude of approximately 12 mmHg, which is significantly higher than the 2.5 mmHg in the brachial setup computed with the same stiffness parameters. Figure 20a) shows the simulated OMWE along with an example measurement. The maximum amplitude of the measured OMWE is only 50% of the simulated one, which is likely caused by multiple factors. The friction of the piston, suboptimal pressure coupling and variation in the artery dimensions. Nevertheless, the transfer of pulsation from the artery to the sensor is significantly higher in the finger than the upper arm. The model also shows the variation in pulse morphology at different P_t. At negative P_t, the pulse exhibits a 'spiky' shape and at positive P_t the pulses appear wider and softer. This is due to the nonlinear characteristic of the $P_t - V$ curve, as seen in Figure 20.

5.3 Continuous BP monitoring

VUT devices use highly complex and expensive pneumatics for high-frequency control of vascular unloading. We developed a simpler, yet effective technique for continuous BP monitoring. The technique is based on the finding that the non-pulsatile (DC) component of the PPG correlates with both BP and contact pressure. A PPG signal is essentially a composite of two separable components: alternating current (AC) and direct current (DC) components [18]. The AC component corresponds to the pulsatile blood flow in the artery and the DC component is considered to probe the nonpulsatile composite of the steady venous and arterial blood volume in the underlying tissue. A study comparing intra-arterial BP to a PPG signal showed a clear

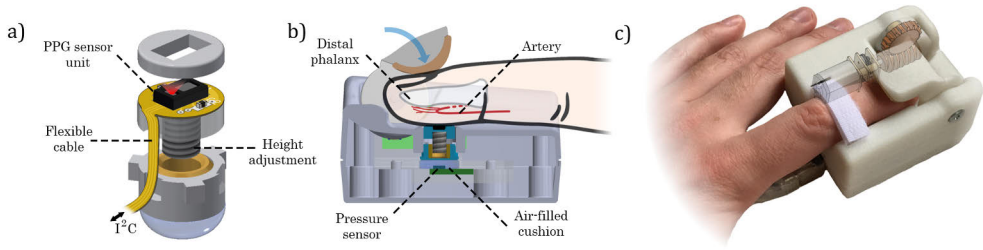

Figure 21. Mechanics for Instrument IIIa. a) Piston construction is similar to Instrument IIIb, with a PPG sensor added. A custom PCB was manufactured for this purpose. b) Half section view of the instrument, showing the targeted artery in the fingertip. c) A photograph of the device in use, with the inner power train highlighted. Figure adapted from [14]

correlation between BP and the PPG DC component.

Our method relies on keeping the DC component of the infrared (IR) PPG signal constant by altering the applied external pressure using an electronic feedback mechanism. We used the miniaturized Instrument IIIb as the base for the study and added a PPG sensor on top of the sensing piston. In addition, the firmware was modified to implement the feedback mechanism used for continuous BP. Since the proposed method does not need to control the contact pressure hundreds of times in a second, we are able to use a pressing mechanism based on a DC motor. This also removes the need for an inflatable cuff, making the technique cuffless.

5.3.1 Low-frequency vascular unloading technique

Operation of the device can be divided into two segments: open-loop action and closed-loop action. Open-loop action is responsible for the calibration phase, and is mostly done at the PC software end. Closed-loop action is responsible for the continuous BP acquisition phase. The computation for the close-loop phase is independently performed at the device microcontroller unit.

Open-loop action

In order to find the correct volume clamping pressure, the method relies on an initial calibration used to find the initial setpoint. This is found at the level of zero transmural pressure (P_t). At this point, the transfer of the pulsatile signal to the sensor is at its maximum. The setpoint is found using open-loop control. Similar to the oscillometric method, the contact pressure is increased and the pressure ramp is stopped when reaching suprasystolic pressure (140 mmHg in most cases). The point of maximum pulsation in the pressure curve is found from the oscillogram. This marks the level of finger mean arterial pressure ($\text{MAP}_{\text{finger}}$) and zero P_t. The contact pressure is then

set to this level and the desired setpoint is calculated by computing the mean dc level from five subsequent IR PPG pulses. At the beginning of a measurement, a brachial cuff measurement is taken and the pressure signal is calibrated to the brachial MAP provided by the reference device.

Closed-loop action

Following the open-loop phase, the system proceeds to the actual BP tracking phase, which uses a closed-loop feedback system. The system is “closed” since it uses a feedback signal from the output to adjust its performance. Traditional volume clamp systems control the volume between and during each cardiac cycle, which is called ”unloading the artery”. This means that the IR PPG volume is kept constant during the periodic changes, within and across cardiac cycles, caused by pulsatile blood flow. The controller samples the volume hundreds of times during each pulse, resulting in high-frequency feedback. Instead of controlling the volume of each full cardiac cycle, in our method, only the average volume over a cardiac cycle is controlled and kept at a constant level. This is accomplished by taking the mean value of each cardiac cycle and making only one volume compensating maneuver once in a cardiac cycle. Doing this, the AC component of the PPG is left unchanged, and only the DC component is controlled. This low-frequency vascular unloading is much less computationally intensive than traditional VUT and does not require fast manipulation of the contact pressure. After a pulse is detected, the DC value is computed for the pulse by performing numerical integration over one cardiac cycle. The DC level is passed to the controller after each detected pulse and the controller refresh rate is much slower than in traditional VUT. It is actually the same as the heart rate, and not dependent on the sensor sampling frequency. A proportional-integral-derivative (PID) controller is used to modify the counter pressure directed to the finger by keeping the DC level of the IR PPG signal constant. This allows the pressure sensed at the sensor piston to follow mean intra-arterial pressure. Operation of the feedback system is shown in Figure 23.

5.3.2 Vasomotor compensation

We did not implement any real-time setpoint correcting methods, which makes the measurement prone to errors due to possible changes in vasomotor tone. We aimed to solve this by devising a method for recognizing and compensating for these changes. Vasomotor compensation is done in post-processing and no interruptions to the measurement are required. From previous literature, IR and red wavelengths in PPG are known to probe the volume of the large conduit arteries [26]. However, green PPG is known to penetrate the tissue much more superficially, probing arteriolar and capillary circulation [26]. Arterioles are the vessels between arteries and capillaries

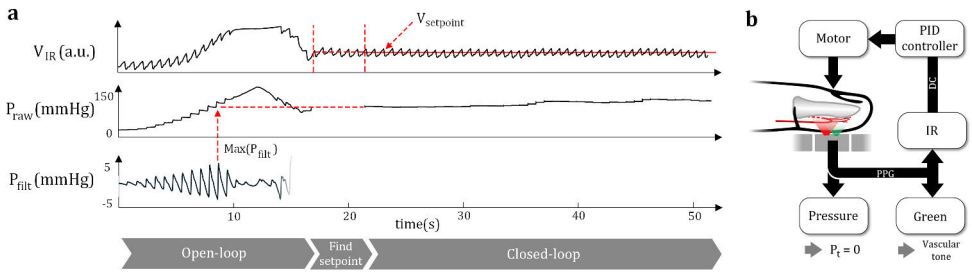

Figure 22. Operating principle of Instrument IIIa. a) The figure shows the open and closed-loop phases of the continuous BP measurement. V_{IR} is the volumetric signal obtained from IR PPG, P_{raw} is the unfiltered pressure signal, and P_{filt} is the highpass filtered pressure signal. The setpoint V_{setpoint} is found by performing an increasing pressure ramp and finding the point of maximum pulsations and setting the contact pressure to the corresponding level. b) System diagram of the device. Figure adapted from [14]

responsible for the majority of vasomotor tone activity[23]. When clamping the arterial volume via IR PPG, the arteriolar/capillary volume is allowed to vary freely to an extent. We believe that this can be observed in the green PPG DC component, where vasodilation accounts for an upward shift in the DC level, and vice versa for vasoconstriction. We demonstrated the ability of green PPG to track vasomotor action by extracting the green DC component, multiply it by a constant k and summing it to the original pressure signal. k was the same in each measurement found empirically.

5.3.3 Blood pressure measurements

First we studied the effect of the feedback mechanism on the morphology of the pulse wave. IR PPG signal was recorded with the subject's hand held at three different heights in respect to the heart level (-10 cm, 0 cm and 10 cm). The measurement was performed both with and without the feedback mechanism. With the feedback loop on, the waveform remained very similar at each height, indicating that P_t remains the same. Correspondingly, with the feedback loop switched off, the height adjustment resulted in a significant change in the pulse morphology. These results are shown in Figure 23a and b. For experimental validation, the ability to maintain zero P_t for continuous tracking of MAP was assessed by comparing simultaneous recordings with the proposed device and the VUT reference device. The measurements were analyzed by dividing each measurement into 10 s epochs and computed the mean for each segment for both devices. Comparing data from each device resulted in (mean$\pm$SD) mmHg of (0.3$\pm$4.3) mmHg for MAP. The subjects were asked to perform certain BP altering maneuvers, such as deep or fast breathing and passive leg raise test. The measured MAP followed the reference very closely during the BP-altering maneuvers. An example is shown in Figure 23c, where the abrupt decrease

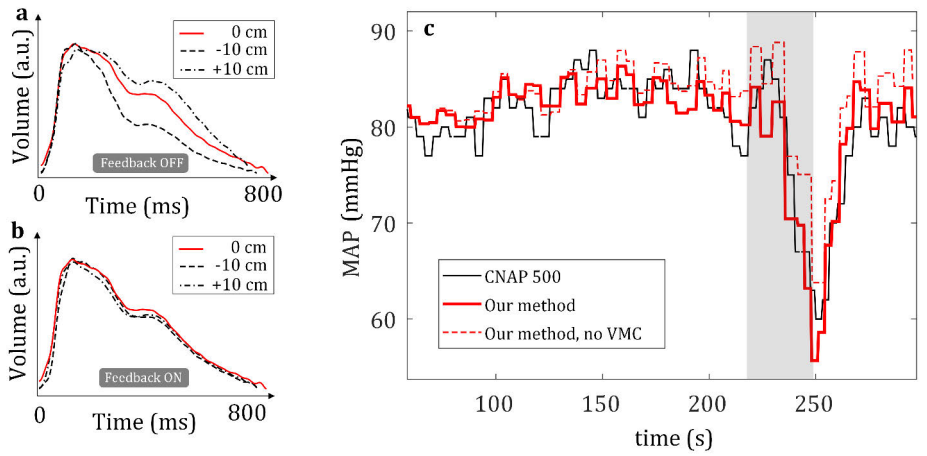

Figure 23. Results from human study III. a) and b) Pulse morphology analysis during pressure changes with (a) and without (b) closed-loop feedback. Each curve represents an ensemble averaged pulse waveform at a certain height (-10 cm, 0 cm and 10 cm) from the heart level. Figure adapted from [14]

in BP caused by fast breathing was as high as 20 mmHg, happening over a time of 15 s. The feedback mechanism was able to react to these relatively fast changes. In most cases, the changes in BP would presumably rarely be faster than these, particularly for home use. However, in an intensive care environment the changes can often be more dramatic.

To study the effect of the vasomotor compensation method to measurement accuracy, we then compared the (mean$\pm$SD) mmHg values of the measurements with and without vasomotor compensation. The one with vasomotor compensation showed better accuracy: (0.3$\pm$4.3) mmHg compared to the original: (-1.4$\pm$5.1) mmHg. This suggests that the green PPG DC signal indeed holds information of the vasomotor process.

6 Discussion

This thesis summarizes the results of five journal articles regarding the design, implementation and validation of new hemodynamic monitoring applications. The accuracy of measuring intermittent BP was comparable with the emerging wearable devices on the market and research endeavours, such as the Omron Heartguide and the smartphone oscillometric finger pressing method. Regarding continuous non-invasive BP monitoring, the proof-of-concept human study in Publication III showed that the proposed technology can achieve similar performance compared with state-of-the-art VUT monitors, such as the CNSystems CNAP500 and CNAP2GO. Nevertheless, a comprehensive study with an intra-arterial reference is justified.

6.1 Achievement of the aims

The results of the five publications I-V showed great promise in the field of wearable BP monitoring. We were able to achieve the aims set for each study and gain deeper knowledge of the mechanisms as well as possibilities in wearable hemodynamic monitoring. Publication I showed that arterial pulse monitoring via pressure sensing is indeed viable. However, this type of approach has a major setback, since it does not allow the measurement of absolute BP. Only relative changes and pulse waveform can be obtained. Publications II and IV addressed this issue and provided a method that can also measure the absolute BP via tono-oscillometry. Although, this results in the need for more complex mechanics and inherently a larger form factor. The miniaturization process proposed in publication III did facilitate this issue. While the overall human study size for intermittent BP monitoring (n=76) was significant, it still falls behind the requirement for the current ISO standard (n=85) [63]. Moreover, the protocol used did not fully meet the standard requirements in terms of BP ranges. On the other hand, if commercialized, the device would have to go through a thorough validation again despite the initial validation. The same applies to the continuous BP monitoring device introduced in publication II. Being a continuous-type monitor it would have to be validated according to the appropriate standard protocol [66]. Finally, publication V fulfilled its aims, summarizing the results from the clinical trials II and IV, along with deepening the understanding of the technology via mathematical modeling.

6.2 Technological feasibility of fingertip BP monitoring

We wanted to receive opinions on the fingertip BP monitoring technology from both the general public and healthcare professionals. Two survey studies were conducted during the project by Taloustutkimus Oy and Clinius Oy in Finland. The first study was an internet survey consisting of multiple different question regarding the use of home BP monitoring and receptivity for fingertip BP monitoring. The survey was done on Finnish adults (n=959) from the ages of 30 years to 79 years. The results showed that nearly all people having a hypertension diagnosis own and frequently use an automated BP monitor. However, in people that are not diagnosed with hypertension only 50% own and less than half of them use a home BP monitor. The most common reason for this was the perception of being healthy and not needing to monitor their BP. Of all subjects, 56% were interested in home BP monitoring and even roughly half of those who do not actively monitor their BP showed interest. 30% of people reported owning a smart device intended for health monitoring (e.g. a smartwatch or a smart ring). The prevalence of smart devices was two times higher in people under 60 years old. There was a high positive correlation between interest for BP monitoring and interest for smart devices. This suggests that the market for smart BP monitoring solutions will increase in the future.

The survey also included a Conjoint analysis part where different factors affecting the appeal of a fingertip BP monitors were assessed. This type of study involves presenting individuals with multiple product or service options and asking them to make trade-offs [111]. We found that people were interested in a subscription based model where different analysis options are provided. These include monitoring arterial health, sleep cycles, stress and oxygen saturation. 36% of general public showed interest in continuous BP monitoring and only 9% wanted a spot measurement device.

The second survey was intended for healthcare professionals and was done as a telephone interview. The survey involved the interest for fingertip BP monitoring. Eight professionals (4 females) were interviewed of whom four were specialist medical doctors and four were registered nurses. Nearly all interviewees suggested that traditional brachial cuff monitors are inconvenient for both the healthcare professional and the patient, and hoped that the fingertip monitor could solve these issues, including pain and the need to remove clothing. The need for a device to measure BP conveniently in elderly people was highlighted. It was reported that the absolute accuracy in some cases such as ambulatory and ICU monitoring, is not the priority, but to be able to detect adverse changes, such as a sudden drop in BP. One of the interviewees noted an interesting use case for monitoring patients that experience a significant drop in BP after e.g. vaccination or drug administration. For this, a finger-worn device that can detect abrupt changes in BP could prove useful. The interviewees also raised questions on the reliability of fingertip BP monitoring. Problems in

finger vasculature in the elderly and issues with the device moving in the finger were discussed.

We also recognize the concerns raised above. Poor finger vasculature and in many cases cold fingers can cause inaccuracy. However, during human study IV, we were able to recruit a reasonable amount of elderly subjects with various health conditions, and the technique was able to perform well. The fear of the device performing poorly outside the initial healthy test group was alleviated during the study. We also received supportive feedback from the subjects which drove us to further develop the technology.

6.3 Future directions

Since the technologies presented show potential, they definitely deserve to be further studied and refined. There are a couple of crucial decisions to be made when continuing the project.

From a more commercial perspective, the first question is whether to target the device to personal health monitoring or to make the decision to enter the clinical device market. The home monitoring or smart wearable market has huge potential but is dominated by certain big operators. The challenge in pursuing the clinical diagnostic device market is the rigor validations and clearances one has to go through before being able to even enter the market.

The second factor to consider is whether to continue with the spot BP monitoring or to lean into truly continuous monitoring. This also dictates the form factor to an extent. Intermittent BP monitoring is adequate in most cases and can be used to obtain time-series data, similar to continuous monitoring, only having worse temporal resolution. Here, the importance of accuracy is pronounced, while in continuous monitoring the ability to pick up fast changes in BP is crucial.

A pulse oximeter type design could prove to be the most viable, since it is already widely adapted in clinical use and thus we would not need any additional devices connected to the patient. Moreover, the need for a brachial cuff would be eliminated.

The tono-oscillometric method introduced in this thesis was adapted in our multi-wavelength PPG proof-of-concept study [17]. Our aim was to shed light into the hemodynamics of microcirculation in the skin by using multiple LEDs with different wavelengths and thus optical penetration depths. The study gave us insights of the BP as well as vasomotor phenomena of microvascular arteries. This direction of research shows great promise and via this technology we hope to be able to understand the mechanism in different cardiovascular diseases.

7 Conclusion

The worldwide market for home blood pressure monitoring is anticipated to surpass 5.5 billion USD by 2030, with an annual growth rate of 6.85% from 2023 to 2030 [112]. The global rise in the prevalence of hypertension and cardiovascular diseases, along with governmental control, are key drivers in the healthcare industry. Digital BP monitors designed for home use account for 64.3% of the market, with Omron Healthcare leading as the primary manufacturer [113]. Arm-based digital BP monitors are the most common type. However, wrist monitors are anticipated to gain popularity due to their capability for multi-parameter readings and integration with smartphones [114].

In this thesis, a new BP monitoring technology from the fingertip was conceived and implemented as well as validated in several clinical studies, done in collaboration with the Turku University hospital. Publication I addressed the need for wearable pressure sensor based pulse wave monitoring and showed its capabilities in human study I. The results collected from publication I showed the need and paved the way for a calibration-free BP measurement technology utilizing state-of-the-art MEMS technology and mechatronics. Publication II introduced a working prototype of a tono-oscillometric monitor and provided proof-of-concept validation for it in human study II. The technology was further refined in two continuation studies. The technology from publication II was miniaturized and implemented in a wearable pulse oximeter type form factor. In publication III, the technology was harnessed for use in continuous BP monitoring by adding an optical sensing modality into the device. This resulted in the application of low-frequency vascular unloading technology, which was tested in human study III. In publication IV the miniaturization process was explained in detail and the system was again validated in human study IV. Cost-effectiveness is definitely a key factor in making the technology available for the wider public and this was achieved by using mostly off-the-shelf components and modifying them for the intended use. Finally, in publication IV, we make use of the efforts made before and draw new conclusions based on the combined data.

Fingertip monitoring has already been in wide use in the form of clinical pulse oximeters which makes the technology reported in this work desirable. Being able to measure BP from the fingertip along with oxygen saturation would eliminate the need for an additional arm cuff in the ICU. The wearable form factor also enables minimally intrusive measurement, which is important for example during sleep. Night-

time – or nocturnal – BP variation has been found to provide a more accurate profile of cardiovascular health than standard office BP [115]. Using the device introduced in publication III, continuous acquisition of BP should be possible during night-time. If a less temporally accurate measurement is sufficient, intermittent measurement as described in publication IV could prove useful, still portraying the long-time variations in BP.

List of References

[1] *Hypertension.* World Health Organization, Accessed on: April 2021 [Online], Available: https://www.who.int/news-room/fact-sheets/detail/hypertension.

[2] Mohammad H. Forouzanfar, Patrick Liu, Gregory A. Roth, Marie Ng, Stan Biryukov, Laurie Marczak, Lily Alexander, Kara Estep, Kalkidan Hassen Abate, Tomi F. Akinyemiju, Raghib Ali, Nelson Alvis-Guzman, Peter Azzopardi, Amitava Banerjee, Till Bärnighausen, Arindam Basu, Tolesa Bekele, Derrick A. Bennett, Sibhatu Biadgilign, Ferrán Catalá-López, Valery L. Feigin, Joao C. Fernandes, Florian Fischer, Alemseged Aregay Gebru, Philimon Gona, Rajeev Gupta, Graeme J. Hankey, Jost B. Jonas, Suzanne E. Judd, Young-Ho Khang, Ardeshir Khosravi, Yun Jin Kim, Ruth W. Kimokoti, Yoshihiro Kokubo, Dhaval Kolte, Alan Lopez, Paulo A. Lotufo, Reza Malekzadeh, Yohannes Adama Melaku, George A. Mensah, Awoke Misganaw, Ali H. Mokdad, Andrew E. Moran, Haseeb Nawaz, Bruce Neal, Frida Namnyak Ngalesoni, Takayoshi Ohkubo, Farshad Pourmalek, Anwar Rafay, Rajesh Kumar Rai, David Rojas-Rueda, Uchechukwu K. Sampson, Itamar S. Santos, Monika Sawhney, Aletta E. Schutte, Sadaf G. Sepanlou, Girma Temam Shifa, Ivy Shiue, Bemnet Amare Tedla, Amanda G. Thrift, Marcello Tonelli, Thomas Truelsen, Nikolaos Tsilimparis, Kingsley Nnanna Ukwaja, Olalekan A. Uthman, Tommi Vasankari, Narayanaswamy Venketasubramanian, Vasiliy Victorovich Vlassov, Theo Vos, Ronny Westerman, Lijing L. Yan, Yuichiro Yano, Naohiro Yonemoto, Maysaa El Sayed Zaki, and Christopher J. L. Murray. Global Burden of Hypertension and Systolic Blood Pressure of at Least 110 to 115 mm Hg, 1990-2015. JAMA*, 317(2):165–182, 01 2017. ISSN 0098-7484. doi: 10.1001/jama.2016.19043.*

[3] Suzanne Oparil, Maria Czarina Acelajado, George L. Bakris, Dan R. Berlowitz, Renata Cífková, Anna F. Dominiczak, Guido Grassi, Jens Jordan, Neil R. Poulter, Anthony Rodgers, and Paul K. Whelton. Hypertension. Nature Reviews Disease Primers*, 4(1):18014, Mar 2018. ISSN 2056-676X. doi: 10.1038/nrdp.2018.14.*

[4] Joshua D Bundy, Changwei Li, Patrick Stuchlik, Xiaoqing Bu, Tanika N Kelly, Katherine T Mills, Hua He, Jing Chen, Paul K Whelton, and Jiang He. Systolic blood pressure reduction and risk of cardiovascular disease and mortality: a systematic review and network meta-analysis. JAMA cardiology*, 2(7):775–*

781, 2017.

[5] Albert L Siu. Screening for high blood pressure in adults: Us preventive services task force recommendation statement. Annals of internal medicine*, 163 (10):778–786, 2015.*

[6] Paul Muntner, Daichi Shimbo, Robert M Carey, Jeanne B Charleston, Trudy Gaillard, Sanjay Misra, Martin G Myers, Gbenga Ogedegbe, Joseph E Schwartz, Raymond R Townsend, et al. Measurement of blood pressure in humans: a scientific statement from the american heart association. Hypertension*, 73(5):e35–e66, 2019.*

[7] John M. Flack and Bemi Adekola. Blood pressure and the new acc/aha hypertension guidelines. Trends in Cardiovascular Medicine*, 30(3): 160–164, 2020. ISSN 1050-1738. doi: https://doi.org/10.1016/j.tcm. 2019.05.003. URL* https://www.sciencedirect.com/science/article/pii/S1050173819300684*.*

[8] Dylan M Bard, Jeffrey I Joseph, and Noud van Helmond. Cuff-less methods for blood pressure telemonitoring. Frontiers in cardiovascular medicine*, 6(40), 2019.*

[9] James E Sharman, Isabella Tan, George S Stergiou, Carolina Lombardi, Francesca Saladini, Mark Butlin, Raj Padwal, Kei Asayama, Alberto Avolio, Tammy M Brady, et al. Automated 'oscillometric'blood pressure measuring devices: how they work and what they measure. Journal of human hypertension*, 37(2):93–100, 2023.*

[10] Matti Kaisti, Tuukka Panula, Joni Leppänen, Risto Punkkinen, Mojtaba Jafari Tadi, Tuija Vasankari, Samuli Jaakkola, Tuomas Kiviniemi, Juhani Airaksinen, Pekka Kostiainen, et al. Clinical assessment of a non-invasive wearable mems pressure sensor array for monitoring of arterial pulse waveform, heart rate and detection of atrial fibrillation. NPJ digital medicine*, 2(1):39, 2019.*

[11] Tuukka Panula, Tero Koivisto, Mikko Pänkäälä, Teemu Niiranen, Ilkka Kantola, and Matti Kaisti. An instrument for measuring blood pressure and assessing cardiovascular health from the fingertip. Biosensors and Bioelectronics*, 167:112483, 2020.*

[12] Tuukka Panula, Juuso Blomster, Mikko Pänkäälä, Tero Koivisto, and Matti Kaisti. An automated device for recording peripheral arterial waveform. In 2019 Computing in Cardiology (CinC)*, pages Page–1. IEEE, 2019.*

[13] Tuukka Panula, Jukka-Pekka Sirkiä, and Matti Kaisti. Continuous blood pressure monitoring using non-pulsatile photoplethysmographic components for low-frequency vascular unloading. IEEE Transactions on Instrumentation and Measurement*, 2023.*

[14] Tuukka Panula, Jukka-Pekka Sirkiä, and Matti Kaisti. Control method for continuous non-invasive arterial pressure monitoring using the non-pulsatile com-

ponent of the ppg signal. In 2021 Computing in Cardiology (CinC)*, volume 48, pages 1–4. IEEE, 2021.*

[15] Tuukka Panula, Jukka-Pekka Sirkiä, Tero Koivisto, Mikko Pänkäälä, Teemu Niiranen, Ilkka Kantola, and Matti Kaisti. Development and clinical validation of a miniaturized finger probe for bedside hemodynamic monitoring. Iscience*, 26(11), 2023.*

[16] Tuukka Panula, Jukka-Pekka Sirkiä, and Matti Kaisti. Miniaturization of a finger-worn blood pressure instrument. In 2021 43rd Annual International Conference of the IEEE Engineering in Medicine & Biology Society (EMBC)*, pages 7441–7444. IEEE, 2021.*

[17] Jukka-Pekka Sirkia, Tuukka Panula, and Matti Kaisti. Tonometric multi-wavelength photoplethysmography for studying the cutaneous microvasculature of the fingertip. IEEE Transactions on Instrumentation and Measurement*, 2023.*

[18] Ramakrishna Mukkamala, Jin-Oh Hahn, Omer T Inan, Lalit K Mestha, Chang-Sei Kim, Hakan Töreyin, and Survi Kyal. Toward ubiquitous blood pressure monitoring via pulse transit time: theory and practice. IEEE Transactions on Biomedical Engineering*, 62(8):1879–1901, 2015.*

[19] Mohamed Elgendi, Richard Fletcher, Yongbo Liang, Newton Howard, Nigel H Lovell, Derek Abbott, Kenneth Lim, and Rabab Ward. The use of photoplethysmography for assessing hypertension. NPJ digital medicine*, 2(60), 2019.*

[20] Xiao-Rong Ding, Ni Zhao, Guang-Zhong Yang, Roderic I Pettigrew, Benny Lo, Fen Miao, Ye Li, Jing Liu, and Yuan-Ting Zhang. Continuous blood pressure measurement from invasive to unobtrusive: celebration of 200th birth anniversary of carl ludwig. IEEE journal of biomedical and health informatics*, 20(6): 1455–1465, 2016.*

[21] Gbenga Ogedegbe and Thomas Pickering. Principles and techniques of blood pressure measurement. Cardiology clinics*, 28(4):571–586, 2010.*

[22] Tuukka Panula, Jukka-Pekka Sirkiä, David Wong, and Matti Kaisti. Advances in non-invasive blood pressure measurement techniques. IEEE Reviews in Biomedical Engineering*, 16:424–438, 2022.*

[23] Leslie Alexander Geddes. Handbook of blood pressure measurement*. Springer Science & Business Media, 2013.*

[24] Hiroshi Miyashita. Clinical assessment of central blood pressure. Current hypertension reviews*, 8(2):80–90, 2012.*

[25] Mohamad Forouzanfar, Hilmi R Dajani, Voicu Z Groza, Miodrag Bolic, Sreeraman Rajan, and Izmail Batkin. Oscillometric blood pressure estimation: past, present, and future. IEEE reviews in biomedical engineering*, 8:44–63, 2015.*

[26] AS Iberall. Anatomy and steady flow characteristics of the arterial system with an introduction to its pulsatile characteristics. Mathematical Biosciences*, 1 (3):375–395, 1967.*

[27] *George S Stergiou, Paolo Palatini, Roland Asmar, John P Ioannidis, Anastasios Kollias, Peter Lacy, Richard J McManus, Martin G Myers, Gianfranco Parati, Andrew Shennan, et al. Recommendations and practical guidance for performing and reporting validation studies according to the universal standard for the validation of blood pressure measuring devices by the association for the advancement of medical instrumentation/european society of hypertension/international organization for standardization (aami/esh/iso).* Journal of Hypertension, *37(3):459–466, 2019.*

[28] *Jeremy Booth. A short history of blood pressure measurement.* Proc roy Soc Med, *70:793–799, 1977.*

[29] *L. Peter, N. Noury, and M. Cerny. A review of methods for non-invasive and continuous blood pressure monitoring: Pulse transit time method is promising?* IRBM, *35(5):271 – 282, 2014. ISSN 1959-0318. doi: https://doi.org/10.1016/j.irbm.2014.07.002.*

[30] *Jo Anna M Shimek, Jorge Emmanuel, Peter Orris, Yves Chartier, World Health Organization, et al. Replacement of mercury thermometers and sphygmomanometers in health care: technical guidance. Technical report, World Health Organization, 2011.*

[31] *John N Amoore. Extracting oscillometric pulses from the cuff pressure: does it affect the pressures determined by oscillometric blood pressure monitors?* Blood pressure monitoring, *11(5):269–279, 2006.*

[32] *Jiankun Liu, Jin-Oh Hahn, and Ramakrishna Mukkamala. Error mechanisms of the oscillometric fixed-ratio blood pressure measurement method.* Annals of biomedical engineering, *41(3):587–597, 2013.*

[33] *Anand Chandraskehar, Mohammad Yavarimanesh, Jin-Oh Hahn, Shih-Hsien Sung, Chen-Huan Chen, Hao-Min Cheng, and Ramakrishna Mukkamala. Formulas to explain popular oscillometric blood pressure estimation algorithms.* Frontiers in Physiology, *10:1415, 2019.*

[34] *Jiankun Liu, Hao-Min Cheng, Chen-Huan Chen, Shih-Hsien Sung, Mohsen Moslehpour, Jin-Oh Hahn, and Ramakrishna Mukkamala. Patient-specific oscillometric blood pressure measurement.* IEEE Transactions on Biomedical Engineering, *63(6):1220–1228, 2015.*

[35] *Charles F Babbs. Oscillometric measurement of systolic and diastolic blood pressures validated in a physiologic mathematical model.* Biomedical engineering online, *11(1):1–22, 2012.*

[36] *Karen Soueidan, Silu Chen, Hilmi R Dajani, Miodrag Bolic, and Voicu Groza. Augmented blood pressure measurement through the noninvasive estimation of physiological arterial pressure variability.* Physiological measurement, *33(6):881, 2012.*

[37] *J. Liu, C. G. Sodini, Y. Ou, B. Yan, Y. T. Zhang, and N. Zhao. Feasibility of fingertip oscillometric blood pressure measurement: Model-based analysis*

and experimental validation. IEEE Journal of Biomedical and Health Informatics*, 24(2):533–542, Feb 2020. ISSN 2168-2208. doi: 10.1109/JBHI.2019.2919896.*

[38] Gary M. Drzewiecki, Julius Melbin, and Abraham Noordergraaf. Arterial tonometry: Review and analysis. Journal of Biomechanics*, 16(2):141–152, 1983. ISSN 0021-9290. doi: https://doi.org/10.1016/0021-9290(83)90037-4.*

[39] Ruiping Wang, Wenyan Jia, Zhi-Hong Mao, Robert J. Sclabassi, and Mingui Sun. Cuff-free blood pressure estimation using pulse transit time and heart rate. International conference on signal processing proceedings. International Conference on Signal Processing*, 2014:115–118, Oct 2014. doi: 10.1109/ICOSP.2014.7014980.*

[40] Yinji Ma, Jungil Choi, Aurélie Hourlier-Fargette, Yeguang Xue, Ha Uk Chung, Jong Yoon Lee, Xiufeng Wang, Zhaoqian Xie, Daeshik Kang, Heling Wang, Seungyong Han, Seung-Kyun Kang, Yisak Kang, Xinge Yu, Marvin J. Slepian, Milan S. Raj, Jeffrey B. Model, Xue Feng, Roozbeh Ghaffari, John A. Rogers, and Yonggang Huang. Relation between blood pressure and pulse wave velocity for human arteries. Proceedings of the National Academy of Sciences*, 115 (44):11144–11149, 2018. ISSN 0027-8424. doi: 10.1073/pnas.1814392115. URL* `https://www.pnas.org/content/115/44/11144`*.*

[41] Stephane Laurent, John Cockcroft, Luc Van Bortel, Pierre Boutouyrie, Cristina Giannattasio, Daniel Hayoz, Bruno Pannier, Charalambos Vlachopoulos, Ian Wilkinson, and on behalf of the European Network for Non-invasive Investigation of Large Arteries Struijker-Boudier, Harry. Expert consensus document on arterial stiffness: methodological issues and clinical applications. European Heart Journal*, 27(21):2588–2605, 09 2006. ISSN 0195-668X. doi: 10.1093/eurheartj/ehl254. URL* `https://doi.org/10.1093/eurheartj/ehl254`*.*

[42] Heiko Gesche, Detlef Grosskurth, Gert Küchler, and Andreas Patzak. Continuous blood pressure measurement by using the pulse transit time: comparison to a cuff-based method. European Journal of Applied Physiology*, 112(1):309–315, Jan 2012. ISSN 1439-6327. doi: 10.1007/s00421-011-1983-3.*

[43] Y. Chen, C. Wen, G. Tao, and M. Bi. A new methodology of continuous and noninvasive blood pressure measurement by pulse wave velocity. In 2010 11th International Conference on Control Automation Robotics Vision*, pages 1018–1023, 2010. doi: 10.1109/ICARCV.2010.5707813.*

[44] Teemu Koivistoinen, Leo-Pekka Lyytikäinen, Heikki Aatola, Tiina Luukkaala, Markus Juonala, Jorma Viikari, Terho Lehtimäki, Olli T Raitakari, Mika Kähönen, and Nina Hutri-Kähönen. Pulse wave velocity predicts the progression of blood pressure and development of hypertension in young adults. Hypertension*, 71(3):451–456, 2018.*

[45] A. I. Moens. Die Pulscurve*. E. J. Brill, Leiden, 1878.*

[46] *D. J. Korteweg. Ueber die fortpflanzungsgeschwindigkeit des schalles in elastischen röhren.* Annalen der Physik, *241(12):525–542, 1878. doi: https://doi.org/10.1002/andp.18782411206. URL* https://onlinelibrary.wiley.com/doi/abs/10.1002/andp.18782411206.

[47] *F. J. Callaghan, L. A. Geddes, C. F. Babbs, and J. D. Bourland. Relationship between pulse-wave velocity and arterial elasticity.* Medical and Biological Engineering and Computing, *24(3):248–254, May 1986. ISSN 1741-0444. doi: 10.1007/BF02441620.*

[48] *Xiaorong Ding, Yuanting Zhang, and Hon Ki Tsang. Impact of heart disease and calibration interval on accuracy of pulse transit time–based blood pressure estimation.* Physiological measurement, *37(2), 2016.*

[49] *Solmaz Rastegar, Hamid GholamHosseini, and Andrew Lowe. Non-invasive continuous blood pressure monitoring systems: current and proposed technology issues and challenges.* Physical and Engineering Sciences in Medicine, *43 (1):11–28, 2020.*

[50] *Josep Solà and Ricard Delgado-Gonzalo.* The Handbook of Cuffless Blood Pressure Monitoring. *Springer, 2019.*

[51] *Martin C Baruch, Darren ER Warburton, Shannon SD Bredin, Anita Cote, David W Gerdt, and Charles M Adkins. Pulse decomposition analysis of the digital arterial pulse during hemorrhage simulation.* Nonlinear biomedical physics, *5(1):1–15, 2011.*

[52] *Irwin Gratz, Edward Deal, Francis Spitz, Martin Baruch, I Elaine Allen, Julia E Seaman, Erin Pukenas, and Smith Jean. Continuous non-invasive finger cuff caretaker® comparable to invasive intra-arterial pressure in patients undergoing major intra-abdominal surgery.* BMC anesthesiology, *17(1):1–11, 2017.*

[53] *Ben PM Imholz, Wouter Wieling, Gert A van Montfrans, and Karel H Wesseling. Fifteen years experience with finger arterial pressure monitoring: assessment of the technology.* Cardiovascular research, *38(3):605–616, 1998.*

[54] *Robert D Boehmer. Continuous, real-time, noninvasive monitor of blood pressure: Peňaz methodology applied to the finger.* Journal of clinical monitoring, *3(4):282–287, 1987.*

[55] *J Penaz. Criteria for set point estimation in the volume clamp method of blood pressure measurement.* Physiological research, *41(1):5–10, 1992.*

[56] *Jürgen Fortin, Dorothea E Rogge, Christian Fellner, Doris Flotzinger, Julian Grond, Katja Lerche, and Bernd Saugel. A novel art of continuous noninvasive blood pressure measurement.* Nature communications, *12(1):1–14, 2021.*

[57] *K Jagomägi, J Talts, R Raamat, and E Länsimies. Continuous non-invasive measurement of mean blood pressure in fingers by volume-clamp and differential oscillometric method.* Clinical Physiology, *16(5):551–560, 1996.*

[58] *Kersti Jagomägi, Jaak Talts, Peeter Tähepõld, and Rein Raamat. A comparison of differential oscillometric device with invasive mean arterial blood pressure monitoring in intensive care patients.* Clinical Physiology and Functional Imaging*, 31(3):188–192, 2011.*

[59] *George S Stergiou, Bruce Alpert, Stephan Mieke, Roland Asmar, Neil Atkins, Siegfried Eckert, Gerhard Frick, Bruce Friedman, Thomas Graßl, Tsutomu Ichikawa, et al. A universal standard for the validation of blood pressure measuring devices: Association for the advancement of medical instrumentation/european society of hypertension/international organization for standardization (aami/esh/iso) collaboration statement.* Hypertension*, 71(3):368–374, 2018.*

[60] *George S. Stergiou, Eamon Dolan, Anastasios Kollias, Neil R. Poulter, Andrew Shennan, Jan A. Staessen, Zhen-Yu Zhang, and Michael A. Weber. Blood pressure measurement in special populations and circumstances.* The Journal of Clinical Hypertension*, 20(7):1122–1127, 2018. doi: https://doi.org/10.1111/jch.13296.*

[61] *William B White, Alan S Berson, Carroll Robbins, Michael J Jamieson, L Michael Prisant, Edward Roccella, and Sheldon G Sheps. National standard for measurement of resting and ambulatory blood pressures with automated sphygmomanometers.* Hypertension*, 21(4):504–509, 1993.*

[62] *EO Brien, J Petrie, W Littler, M de Swiet, PL Padfield, DG Altman, M Bland, A Coats, and N Atkins. The british hypertension society protocol for the evaluation of blood pressure devices.* J Hypertens*, 11(Suppl. 2):S43–S62, 1993.*

[63] *Eoin O'Brien, Thomas Pickering, Roland Asmar, Martin Myers, Gianfranco Parati, Jan Staessen, Thomas Mengden, Yutaka Imai, Bernard Waeber, Paolo Palatini, et al. Working group on blood pressure monitoring of the european society of hypertension international protocol for validation of blood pressure measuring devices in adults.* Blood pressure monitoring*, 7(1):3–17, 2002.*

[64] *Ramakrishna Mukkamala, Mohammad Yavarimanesh, Keerthana Natarajan, Jin-Oh Hahn, Konstantinos G Kyriakoulis, Alberto P Avolio, and George S Stergiou. Evaluation of the accuracy of cuffless blood pressure measurement devices: Challenges and proposals.* Hypertension*, 78(5):1161–1167, 2021.*

[65] *IEEE standard for wearable cuffless blood pressure measuring devices.* IEEE Std 1708-2014*, 2014.*

[66] *IEEE standard for wearable, cuffless blood pressure measuring devices - amendment 1.* IEEE Std 1708a-2019 (Amendment to IEEE Std 1708-2014)*, 2019. doi: 10.1109/IEEESTD.2019.8859685.*

[67] *Mitsuo Kuwabara, Kanako Harada, Yukiko Hishiki, and Kazuomi Kario. Validation of two watch-type wearable blood pressure monitors according to the ansi/aami/iso81060-2: 2013 guidelines: Omron hem-6410t-zm and hem-6410t-zl.* The Journal of Clinical Hypertension*, 21(6):853–858, 2019.*

[68] *Edoardo Casiglia, Valérie Tikhonoff, Federica Albertini, and Paolo Palatini. Poor reliability of wrist blood pressure self-measurement at home: a population-based study.* Hypertension*, 68(4):896–903, 2016.*

[69] *Adi Schejter Bar-Noam, Alexander Kaminsky, Albert Bravo, Louis Shenkman, Naomi Nacasch, and Ilya Fine. Novel method for non-invasive blood pressure measurement from the finger using an optical system based on dynamic light scattering. In* European Conference on Biomedical Optics*, number 11075_23. Optical Society of America, 2019.*

[70] *Anand Chandrasekhar, Chang-Sei Kim, Mohammed Naji, Keerthana Natarajan, Jin-Oh Hahn, and Ramakrishna Mukkamala. Smartphone-based blood pressure monitoring via the oscillometric finger-pressing method.* Science translational medicine*, 10(431), 2018.*

[71] *Anand Chandrasekhar, Keerthana Natarajan, Mohammad Yavarimanesh, and Ramakrishna Mukkamala. An iphone application for blood pressure monitoring via the oscillometric finger pressing method.* Scientific reports*, 8(1):13136, 2018.*

[72] *Christopher Elliott, Mark-Eric Jones, Mikhall Nagoga, Shady Gawad, and Gabriel Klein. Personal health data collection, December 31 2015. US Patent App. 14/767,444, [Online] Available: https://patents.google.com/patent/CA2840136A1/en?oq=Personal-health-data-collection.*

[73] *"Accurate blood pressure measurement can now be cuff-less and calibration-free and can be built in to every smartphone, key=Accurate blood pressure measurement can now be cuff-less and calibration-free and can be built in to every smartphone".* Leman Micro Devices, Accessed on: May 2021 [Online], Available: https://www.leman-micro.com/accurate-blood-pressure-measurement-can-now-be-cuff-less-and-calibration-free-and-can-be-built-in-to-every-smartphone.

[74] *D Nair, SY Tan, HW Gan, SF Lim, J Tan, M Zhu, H Gao, NH Chua, WL Peh, and KH Mak. The use of ambulatory tonometric radial arterial wave capture to measure ambulatory blood pressure: the validation of a novel wrist-bound device in adults.* Journal of human hypertension*, 22(3):220–222, 2008.*

[75] *Philipp Krisai, Annina Salome Vischer, Leo Kilian, Andrea Meienberg, Michael Mayr, and Thilo Burkard. Accuracy of 24-hour ambulatory blood pressure monitoring by a novel cuffless device in clinical practice.* Heart*, 105(5):399–405, 2019.*

[76] *Dean Nachman, Yftach Gepner, Nir Goldstein, Eli Kabakov, Arik Ben Ishay, Romi Littman, Yuval Azmon, Eli Jaffe, and Arik Eisenkraft. Comparing blood pressure measurements between a photoplethysmography-based and a standard cuff-based manometry device.* Scientific reports*, 10(1):1–9, 2020.*

[77] *Jakob Nyvad, Kent L Christensen, Niels Henrik Buus, and Mark Reinhard.*

The cuffless somnotouch nibp device shows poor agreement with a validated oscillometric device during 24-h ambulatory blood pressure monitoring. The Journal of Clinical Hypertension*, 23(1):61–70, 2021.*

[78] Timothy B. Plante, Bruno Urrea, Zane T. MacFarlane, Roger S. Blumenthal, III Miller, Edgar R., Lawrence J. Appel, and Seth S. Martin. Validation of the Instant Blood Pressure Smartphone App. JAMA Internal Medicine*, 176(5): 700–702, 05 2016. ISSN 2168-6106. doi: 10.1001/jamainternmed.2016.0157. URL* https://doi.org/10.1001/jamainternmed.2016.0157*.*

[79] Christian Holz and Edward J Wang. Glabella: Continuously sensing blood pressure behavior using an unobtrusive wearable device. Proceedings of the ACM on Interactive, Mobile, Wearable and Ubiquitous Technologies*, 1(3):1–23, 2017.*

[80] Jing Liu, Bryan P Yan, Yuan-Ting Zhang, Xiao-Rong Ding, Peng Su, and Ni Zhao. Multi-wavelength photoplethysmography enabling continuous blood pressure measurement with compact wearable electronics. IEEE Transactions on Biomedical Engineering*, 66(6):1514–1525, 2018.*

[81] Valencell. Internally validated independent results for noninvasive, cuff-less blood pressure estimation utilizing valencell's deep-ppg technology. Technical report, Valencell, Inc., 2020.

[82] Anna Vybornova, Erietta Polychronopoulou, Arlène Wurzner-Ghajarzadeh, Sibylle Fallet, Josep Sola, and Gregoire Wuerzner. Blood pressure from the optical aktiia bracelet: A 1-month validation study using an extended ISO81060-2 protocol adapted for a cuffless wrist device. Blood Pressure Monitoring*, 26(4): 305–311, Aug 2021.*

[83] Patrick Schoettker, Jean Degott, Gregory Hofmann, Martin Proença, Guillaume Bonnier, Alia Lemkaddem, Mathieu Lemay, Raoul Schorer, Urvan Christen, Jean-François Knebel, et al. Blood pressure measurements with the optibp smartphone app validated against reference auscultatory measurements. Scientific Reports*, 10(1):1–12, 2020.*

[84] Hong Luo, Deye Yang, Andrew Barszczyk, Naresh Vempala, Jing Wei, Si Jia Wu, Paul Pu Zheng, Genyue Fu, Kang Lee, and Zhong-Ping Feng. Smartphone-based blood pressure measurement using transdermal optical imaging technology. Circulation: Cardiovascular Imaging*, 12(8):e008857, 2019.*

[85] Ramakrishna Mukkamala. Blood pressure with a click of a camera? Circulation: Cardiovascular Imaging*, 12(8):e009531, 2019. doi: 10.1161/CIRCIMAGING.119.009531. URL* https://www.ahajournals.org/doi/abs/10.1161/CIRCIMAGING.119.009531*.*

[86] Steven F LeBoeuf, Lawrence C Eschbach, Tushar D Tank, Seth E Long, Ryan D Hodges, and Daniel R Moore. Biometric audio earbuds produce cuff-like accuracy in monitoring blood pressure. Journal of the American College of Cardiology*, 75(11S1):3505–3505, 2020.*

[87] *Chih-Cheng Wu and Paul C-P Chao. Ps 05-04 validation of the freescan pulse transit time-based blood pressure monitor.* Journal of Hypertension, *34:e142, 2016.*

[88] *J Solà, A Vybornova, S Fallet, O Grossenbacher, B De Marco, E Olivero, N Siutryk, V Chapuis, and M Bertschi. Aktiia bracelet: monitoring of blood pressure using off-the-shelf optical sensors.* algorithms, *1(6.72):0–7, 2019.*

[89] *Shuran Zhou, Lisheng Xu, Liling Hao, Hanguang Xiao, Yang Yao, Lin Qi, and Yudong Yao. A review on low-dimensional physics-based models of systemic arteries: application to estimation of central aortic pressure.* Biomedical engineering online, *18:1–25, 2019.*

[90] *Jiankun Liu, Hao-Min Cheng, Chen-Huan Chen, Shih-Hsien Sung, Jin-Oh Hahn, and Ramakrishna Mukkamala. Patient-specific oscillometric blood pressure measurement: Validation for accuracy and repeatability.* IEEE journal of translational engineering in health and medicine, *5:1–10, 2016.*

[91] *Kurt Barbe, Wendy Van Moer, and Danny Schoors. Analyzing the windkessel model as a potential candidate for correcting oscillometric blood-pressure measurements.* IEEE Transactions on Instrumentation and Measurement, *61 (2):411–418, 2011.*

[92] *C El-Hajj and Panayiotis A Kyriacou. A review of machine learning techniques in photoplethysmography for the non-invasive cuff-less measurement of blood pressure.* Biomedical Signal Processing and Control, *58:101870, 2020.*

[93] *Fen Miao, Nan Fu, Yuan-Ting Zhang, Xiao-Rong Ding, Xi Hong, Qingyun He, and Ye Li. A novel continuous blood pressure estimation approach based on data mining techniques.* IEEE journal of biomedical and health informatics, *21 (6):1730–1740, 2017.*

[94] *Fan Pan, Peiyu He, Fei Chen, Jing Zhang, He Wang, and Dingchang Zheng. A novel deep learning based automatic auscultatory method to measure blood pressure.* International Journal of Medical Informatics, *128:71–78, 2019.*

[95] *Yongbo Liang, Zhencheng Chen, Rabab Ward, and Mohamed Elgendi. Hypertension assessment via ecg and ppg signals: An evaluation using mimic database.* Diagnostics, *8(65), 2018.*

[96] *Oded Schlesinger, Nitai Vigderhouse, Yair Moshe, and Danny Eytan. Estimation and tracking of blood pressure using routinely acquired photoplethysmographic signals and deep neural networks.* Critical Care Explorations, *2(4), 2020.*

[97] *Hangsik Shin and Se Dong Min. Feasibility study for the non-invasive blood pressure estimation based on ppg morphology: normotensive subject study.* Biomedical engineering online, *16(1), 2017.*

[98] *Jamie Kitt, Rachael Fox, Katherine L Tucker, and Richard J McManus. New approaches in hypertension management: a review of current and developing*

technologies and their potential impact on hypertension care. Current hypertension reports*, 21(6):1–8, 2019.*

[99] Geoffrey H Tison, Avesh C Singh, Daniel A Ohashi, Johnson T Hsieh, Brandon M Ballinger, Jeffrey E Olgin, Gregory M Marcus, and Mark J Pletcher. Cardiovascular risk stratification using off-the-shelf wearables and a multitask deep learning algorithm. Circulation*, 136(suppl_1):A21042–A21042, 2017.*

[100] Brandon Ballinger, Johnson Hsieh, Avesh Singh, Nimit Sohoni, Jack Wang, Geoffrey H Tison, Gregory M Marcus, Jose M Sanchez, Carol Maguire, Jeffrey E Olgin, et al. Deepheart: semi-supervised sequence learning for cardiovascular risk prediction. [Online] Available: arXiv:1802.02511*, 2018.*

[101] Raj Padwal. Cuffless Blood Pressure Measurement: How Did Accuracy Become an Afterthought? American Journal of Hypertension*, 32(9):807–809, 05 2019. ISSN 0895-7061. doi: 10.1093/ajh/hpz070.*

[102] Hidehiko Komine, Yoshiyuki Asai, Takashi Yokoi, and Mutsuko Yoshizawa. Non-invasive assessment of arterial stiffness using oscillometric blood pressure measurement. Biomedical engineering online*, 11(1):1–12, 2012.*

[103] Andreas C Fischer, Fredrik Forsberg, Martin Lapisa, Simon J Bleiker, Göran Stemme, Niclas Roxhed, and Frank Niklaus. Integrating mems and ics. Microsystems & Nanoengineering*, 1(1):1–16, 2015.*

[104] Stefan Keil. Technology and practical use of strain gages: with particular consideration of stress analysis using strain gages*. John Wiley & Sons, 2017.*

[105] A Alvin Barlian, Woo-Tae Park, Joseph R Mallon, Ali J Rastegar, and Beth L Pruitt. Semiconductor piezoresistance for microsystems. Proceedings of the IEEE*, 97(3):513–552, 2009.*

[106] J Martin Bland and DouglasG Altman. Statistical methods for assessing agreement between two methods of clinical measurement. The lancet*, 327 (8476):307–310, 1986.*

[107] Matti Kaisti, Tuukka Panula, Jukka-Pekka Sirkia, Mikko Pankaala, Tero Koivisto, Teemu Niiranen, and Ilkka Kantola. Hemodynamic bedside monitoring instrument with pressure and optical sensors: Validation and modality comparison. Advanced Science*, in production, 2024.*

[108] Chen-Huan Chen, Erez Nevo, Barry Fetics, Peter H Pak, Frank CP Yin, W Lowell Maughan, and David A Kass. Estimation of central aortic pressure waveform by mathematical transformation of radial tonometry pressure: validation of generalized transfer function. Circulation*, 95(7):1827–1836, 1997.*

[109] Robert Looga. The valsalva manoeuvre—cardiovascular effects and performance technique: a critical review. Respiratory physiology & neurobiology*, 147(1):39–49, 2005.*

[110] Berish Strauch and Wilson de Moura. Arterial system of the fingers. The Journal of hand surgery*, 15(1):148–154, 1990.*

[111] Paul E Green, Abba M Krieger, and Yoram Wind. Thirty years of conjoint analysis: Reflections and prospects. Interfaces*, 31(3_supplement):S56–S73, 2001.*

[112] "Global Home Blood Pressure Monitoring Devices Market Size By Product (Sphygmomanometer/Aneroid BP Monitor, Automated/Digital Blood Pressure Monitor, Ambulatory Blood Pressure Monitor), By End-User (Hospitals, Ambulatory Surgical Centers And Clinics, Home Healthcare), By Geographic Scope And Forecast". Verified market research, Accessed on: December 2023 [Online], Available: https://www.https://www.verifiedmarketresearch.com/product/home-blood-pressure-monitoring-devices-market/, .

[113] "Blood Pressure Monitoring Market Size, Share and Industry Analysis By Product Type (Sphygmomanometers, Digital Blood Pressure Monitors, Ambulatory Blood Pressure Monitors), By End User (Hospitals, Ambulatory Surgery Centers & Clinics, Home Healthcare & Others), and Regional Forecast 2018-2025". Fortune Business Insights, Accessed on: January 2022 [Online], Available: https://www.fortunebusinessinsights.com/industry-reports/blood-pressure-monitors-market-100059, .

[114] "Digital Blood Pressure Monitors Market Size, Share and Industry Analysis By Product Type (Arm Type & Wrist Type), End User (Hospitals, Ambulatory Surgical Centers & Clinics, Homecare Settings & Others) and Regional Forecast, 2018 - 2025". Fortune Business Insights, Accessed on: January 2022 [Online], Available: https://www.fortunebusinessinsights.com/industry-reports/digital-blood-pressure-monitors-market-100066, .

[115] Kazuomi Kario, Hiroshi Kanegae, Naoko Tomitani, Yukie Okawara, Takeshi Fujiwara, Yuichiro Yano, Satoshi Hoshide, and J-HOP Study Group. Nighttime blood pressure measured by home blood pressure monitoring as an independent predictor of cardiovascular events in general practice: The j-hop nocturnal blood pressure study. Hypertension*, 73(6):1240–1248, 2019.*

TURUN
YLIOPISTO
UNIVERSITY
OF TURKU

Painosalama, Turku, Finland 2024

ISBN 978-951-29-9792-3 (PRINT)
ISBN 978-951-29-9793-0 (PDF)
ISSN 2736-9390 (PRINT)
ISSN 2736-9684 (ONLINE)